Ⅳ．研究成果の刊行物・別刷

Drug Metab. Pharmacokinet. 20 (4): *SNP27* (300)-*SNP34* (307) (2005).

SNP Communications

Genetic Variations and Haplotypes of CYP2C19 in a Japanese Population

Hiromi FUKUSHIMA-UESAKA[1], Yoshiro SAITO[1,2,*], Keiko MAEKAWA[1,2], Shogo OZAWA[1,3], Ryuichi HASEGAWA[4], Hiroshi KAJIO[5], Nobuaki KUZUYA[5], Kazuki YASUDA[6], Manabu KAWAMOTO[7], Naoyuki KAMATANI[7], Kazuko SUZUKI[8], Tatsuo YANAGAWA[8], Masahiro TOHKIN[1,4] and Jun-ichi SAWADA[1,2]

[1]*Project Team for Pharmacogenetics,* [2]*Division of Biochemistry and Immunochemistry,* [3]*Division of Pharmacology,* [4]*Division of Medicinal Safety Science, National Institute of Health Sciences, Tokyo, Japan* [5]*Division of Endocrine and Metabolic Diseases, the Hospital,* [6]*Department of Metabolic Disorder, Research Institute, International Medical Center of Japan, Toyko, Japan*
[7]*Division of Genomic Medicine, Department of Advanced Biomedical Engineering and Science, Tokyo Women's Medical University, Tokyo, Japan* [8]*Nerima General Hospital, Tokyo, Japan*

Full text of this paper is available at http://www.jstage.jst.go.jp/browse/dmpk

Summary: Forty-eight single nucleotide variations, including 27 novel ones, were found in the 5′-regulatory region, all of the exons and their surrounding introns of *CYP2C19* in 253 Japanese subjects (134 diabetic patients and 119 healthy volunteers). Identified novel variations were as follows: −2772G>A, 2767_−2760delGGTGAACA, −2720T>C, −2547delG, −2545G>T, −2545_−2544 delGC, and −2040C>T in the enhancer region; −778C>T, −777G>A, −529G>C, −189C>A, and −185A>G in the promoter region; 151A>G (S51G), 481G>C (A161P), 986G>A (R329H), 1078G>A (D360N), and 1119C>T (D373D) in the exons, and IVS1+128T>A, IVS3+163G>A, IVS4+271A>G, IVS5−49A>G, IVS6−210C>T, IVS6−196T>A, IVS6−32T>A, IVS7+84G>A, IVS7−174C>T, and IVS8+64C>T in the introns. Since we found no significant differences in the variation frequencies between healthy volunteers and diabetic patients, the data for all subjects were treated as one group in further analysis. The allele frequencies were 0.265 for IVS6−196T>A, 0.045 for −2772G>A and −2720T>C, 0.024 for −2040C>T, 0.014 for IVS7−174C>T, 0.010 for −529G>C, 0.006 for IVS1+128T>A and 481G>C (A161P), 0.004 for −2767_−2760delGGTGAACA and IVS6−210C>T, and 0.002 for the other 17 variations. In addition, the two known nonsynonymous single nucleotide polymorphisms, 681G>A (splicing defect, **2* allele) and 636G>A (W212X; **3* allele) were detected at 0.267 and 0.128 frequencies, respectively. No variation was detected in the known binding sites for constitutive androstane receptor and glucocorticoid receptor. Linkage disequilibrium analysis showed several close linkages of variations throughout the gene. By using the variations, thirty-one haplotypes of *CYP2C19* and their frequencies were estimated. Our results would provide fundamental and useful information for genotyping *CYP2C19* in the Japanese and probably other Asian populations.

Key words: CYP2C19; genetic variation; amino acid alteration; haplotype

On June 13, 2005, these variations were not found on the homepage of the CYP Allele Nomenclature Committee (http://www.imm.ki.se/CYPallele/CYP2C19), the Japanese Single Nucleotide Polymorphisms (JSNP) (http://snp.ims.u-tokyo.ac.jp/), dbSNP in the National Center for Biotechnology Information (http://www.ncbi.nlm.nih.gov/SNP/), or PharmGKB (http://www.pharmgkb.org/do/) database.

This study was supported in part by the Program for the Promotion of Fundamental Studies in Health Sciences, and in part by the Health and Labor Sciences Research Grants from the Ministry of Health, Labor and Welfare.

Received; June 1, 2005, Accepted; July 7, 2005

To whom correspondence should be addressed: Yoshiro SAITO, Ph.D, Division of Biochemistry and Immunochemistry, National Institute of Health Sciences, 1-18-1 Kamiyoga, Setagaya-ku, Tokyo 158-8501, Japan. Tel. +81-3-3700-9453, Fax. +81-3-3707-6950, E-mail: yoshiro@nihs.go.jp

Introduction

In human, cytochrome P450 2C (CYP2C) subfamily consists of four members: CYP2C8, CYP2C9, CYP2C18 and CYP2C19. Their genes are tandemly located on chromosome 10q24.[1] One of the subfamily members, CYP2C19 is a clinically important enzyme that metabolizes a wide variety of drugs, such as antiulcer drugs omeprazole and lansoprazole, an anticonvulsant *S*-mephenytoin, an antidiabetic drug tolbutamide, and an anxiolytic drug diazepam.[2,3] Metabolism of these drugs *in vivo* has been known to be polymorphic, and individuals can be divided into extensive metabolizers and poor metabolizers (PMs). PMs would face higher area under concentration-time curve (AUC) values of the drugs.[4-6] Regarding omeprazole, for example, the PMs show higher cure rates for *Helicobacter pyloli* infection and peptic ulcer because of the higher AUCs, which lead to increased gastric pH and thus are suggested to result in stable antibacterial activity of amoxicillin.[2,4,7]

Ethnic differences in the incidence of PMs among Caucasians (2–5%), Africans (*ca.* 6%) and Asians (13–23%) have been reported.[2,8] These differences are known to be attributed to the genetic polymorphisms of *CYP2C19* gene. de Morais *et al.* first reported the common single nucleotide polymorphisms (SNPs) 681G>A (splicing defect, *CYP2C19*2* allele) and 636G>A (W212X, **3* allele), the latter of which was found only in Japanese but not in Caucasian populations.[9,10] Recent studies showed that the **3* allele is also distributed in Chinese, Thai and Vietnamese with different frequencies.[11] *CYP2C19*2* and **3* generate the null-activity enzyme protein and have been considered to account for >99% of PM alleles in the Japanese population.[10,12] Recently, another minor allele, *CYP2C19*16* (1324C>T, R442C), was found in a Japanese subject who had received mephobarbital (at 0.006 frequency in Japanese population).[13] As for other Asian populations, the two defective alleles *CYP2C19*4* (1A>G, no protein) and **5* (1297C>T, R433W) were also found below 0.005 frequencies in Chinese.[14,15] However, the other alleles (*CYP2C19*6-*15*) have not been detected in Asians.

Recently, the transcriptional regulatory regions of the *CYP2C19* gene were analyzed. Reporter assay with up to 1.8 kb upstream of the 5′-flanking region showed that there were potentially negative and positive elements between 650 to 453 bases and between 224 to 17 bases, respectively, upstream of the translational start site.[16] Furthermore, another report revealed enhancer elements for constitutive androstane receptor (−1891 to −1876 bases from the translational start site) and glucocorticoid receptor (−1750 to −1736).[17]

While the effects of *CYP2C19* polymorphisms have been extensively studied on the **2* and **3* polymorphisms, a comprehensive search for genetic polymorphisms of *CYP2C19* in Asian populations, including the Japanese, is currently lacking. In this study, the 5′-regulatory region, all the exons and their surrounding introns of *CYP2C19* were sequenced in 253 Japanese subjects, and 27 novel variations, including four non-synonymous ones, were identified.

Materials and Methods

Human genomic DNA samples: DNA was extracted from the blood leukocytes of 134 Japanese diabetic patients who had received glimepiride. DNA was also extracted from Epstein-Barr virus-transformed lymphoblastoid cells, which were derived from blood samples collected from 119 healthy Japanese volunteers at the Tokyo Women's Medical University. The ethical review boards of the International Medical Center of Japan, the Nerima General Hospital, the Tokyo Women's Medical University, and the National Institute of Health Sciences approved this study. Written informed consent was obtained from all participating patients as well as all healthy subjects.

Polymerase chain reaction (PCR) conditions for DNA sequencing: First, the multiplex PCR was performed to amplify the entire *CYP2C19* gene by the two mixed primer sets (Mix 1 and Mix 2 in "1st PCR" in **Table 1**). Amplification was performed from 100 ng of genomic DNA using 1.25 units of Ex-Taq (Takara Bio. Inc, Shiga, Japan) with the 0.2 μM of the primers sets. The first PCR conditions were 94°C for 5 min, followed by 30 cycles of 94°C for 30 sec, 60°C for 1 min, and 72°C for 2 min, and then a final extension at 72°C for 7 min. Then each exon was amplified separately using one-fifth volume of the 1st PCR product as a template by Ex-Taq (0.625 units) (Takara Shuzo) with a set of primers (0.2 μM) listed in "2nd PCR" of **Table 1** (designed in the intronic regions). The second-round PCR conditions were 94°C for 5 min, followed by 30 cycles of 94°C for 30 sec, 60°C for 1 min, and 72°C for 2 min, and then a final extension at 72°C for 7 min. Thereafter, the PCR products were treated with a PCR Product Pre-Sequencing Kit (USB Co., Cleveland, OH, USA) and directly sequenced on both strands using an ABI BigDye Terminator Cycle Sequencing Kit (Applied Biosystems, Foster City, CA, USA) with the primers listed in "Sequencing" of **Table 1**. The excess dye was removed by a DyeEx96 kit (Qiagen, Hilden, Germany). The eluates were analyzed on an ABI Prism 3730 DNA Analyzer (Applied Biosystems). All the detected variations were confirmed by repeating the PCR from the genomic DNA and sequencing the newly generated PCR products.

Linkage disequilibrium (LD) and haplotype analysis: Hardy-Weinberg equilibrium and LD analysis was

Table 1. Primer sequences used for the analysis of the *CYP2C19* gene

		Amplified or sequenced region	Forward primer (5′ to 3′)	Reverse primer (5′ to 3′)	Amplified length (bp)
1st PCR	Mix 1	−3k to Exon 1	TTATTTGTTGCTAGGGCTCGTG	CTTACTGTTTACCCTCAGCC	3,281
		Exon 2 to 3	AGGTAGACACAAGAGTGCTGA	TTCTCTGGTGACATGTTCTGGA	1,250
	Mix 2	Exon 4 to 5	CCATTATTTAACCAGCTAGGC	TCCTATCCTGACATCCTTATTG	1,969
		Exon 6	CAAACTATACCAAACAGCAGGCTA	ACTCTACATAGCTTAAAGGGCTCA	6,557
		Exon 7	AATGCTGAAGTGGGTTGTTG	ACCCTGACAGAAATTCTAGCCC	1,272
		Exon 8 to 9	CCCACAACAGTCCCCGAA	CACAAAGGAAGGAAGGTCTAA	3,650
2nd PCR		−3K	TTATTTGTTGCTAGGGCTCGTG	ATCACATCCCGTCTCATAGAA	476
		−2K	CTCAACTTAGCAGAAGAGAGG	CTCATATCCCTTTGGAATCTCT	562
		−1K	AAGCCTTAGTTTCTCAAGCCC	CTTGTTCTCCTTCGTCCCAG	925
		Exon 1	AGAAGACCTCAGCTCAAATCC	CTTACTGTTTACCCTCAGCC	1,249
		Exon 2 to 3	AGGTAGACACAAGAGTGCTGA	TTCTCTGGTGACATGTTCTGGA	1,250
		Exon 4	CCATTATTTAACCAGCTAGGC	AGCCTTGTGAGTAATGGAAGA	727
		Exon 5	AGAAGTCATTTAACTGCTCTGG	TCCTATCCTGACATCCTTATTG	950
		Exon 6	CTCTCTCACCGCTCCTATTCA	GCTGGGATTACAGTGGTGTG	627
		Exon 7	GGTCTTGTTTCTTCATCTAGTCAG	ACCCTGACAGAAATTCTAGCCC	915
		Exon 8	CCCACAACAGTCCCCGAA	GAGGATGTATCACCAGCGGAG	580
		Exon 9	TTGTTTAGTTGCCTATCCATCC	CACAAAGGAAGGAAGGTCTAA	775
Sequencing		−3K	TTATTTGTTGCTAGGGCTCGTG	ATCACATCCCGTCTCATAGAA	
		−2K	CTCAACTTAGCAGAAGAGAGG	CTCATATCCCTTTGGAATCTCT	
		−1K	TGTCTTCTGTTCTCAAAGCATC	CTGAATATATACCACATTCATCC	
		Exon 1	AGGCTGCTGTATTTTTAGTAGG	GACACTGACAGACTGGAAAAGG	
		Exon 2	AGGTAGACACAAGAGTGCTGA	GAGAAACGAAACTAGGAGG	
		Exon 3	GTTTCAGCATCTGTCTTGG	TTCTCTGGTGACATGTTCTGGA	
		Exon 4	CCATTATTTAACCAGCTAGGC	AGCCTTGTGAGTAATGGAAGA	
		Exon 5	AGAGGCTGCTTGATAGAAAT	TCCTATCCTGACATCCTTATTG	
		Exon 6	CTCACCGCTCCTATTCAATATT	AGTGGTGTGCCACAATGC	
		Exon 7	GGTCTTGTTTCTTCATCTAGTCAG	ACCCTGACAGAAATTCTAGCCC	
		Exon 8	CCCACAACAGTCCCCGAA	GAGGATGTATCACCAGCGGAG	
		Exon 9	TTGTTTAGTTGCCTATCCATCC	CACAAAGGAAGGAAGGTCTAA	

performed by SNPAlyze software (Dynacom Co., Yokohama, Japan), and pairwise LD between variations was analyzed by rho square (r^2) values. Some of the haplotypes were unambiguous from subjects with homozygous variations at all sites or a heterozygous variation at only one site. Separately, the diplotype configurations (a combination of haplotypes) were inferred by LDSUPPORT software, which determines the posterior probability distribution of the diplotype configuration for each subject based on the estimated haplotype frequencies.[18] The diplotype configurations of all subjects had a probability (certainty) of more than 0.975 except for 5 subjects. The haplotypes inferred in single subjects are described with haplotype names and a question mark in **Table 3**, since the predictability for these very rare haplotypes is known to be low in some cases. The haplotypes detected in this study were tentatively named as the numbers plus small alphabetical letters, except for the four haplotypes with novel nonsynonymous variations (*CYP2C19*18-*21*), which were registered to the CYP Allele Nomenclature Committe and will be publicized on the committee's Web site.

Results and Discussion

The enhancer (from 2780 to 2350 bases and from 2090 to 1590 bases upstream of the translational start site) and promoter regions (up to 1020 bases upstream of the translational start site), all the 9 exons and their flanking introns of *CYP2C19* were sequenced in 253 Japanese subjects. Genbank accession number NT_030059.12 was utilized for the reference sequence. Forty-eight genetic variations, including 27 novel ones (7 were in the enhancer region, 5 in the promoter region, 5 in the exons and 10 in the introns), were detected (**Table 2**). Since we did not find any significant differences in the frequencies of these variations between healthy volunteers and diabetic patients (by χ^2 test or Fisher's exact test, $P>0.25$), the data for all subjects were analyzed as one group. All of the detected variations were found in Hardy-Weinberg equilibrium ($P \geqq 0.449$).

Four novel nonsynonymous variations, 151A>G (S51G), 481G>C (A161P), 986G>A (R329H) and 1078G>A (D360N), were found as individual heterozygotes at 0.002, 0.006, 0.002 and 0.002 frequencies, respectively (**Fig. 1**). Among them, A161 and D360 are

Table 2. Summary of *CYP2C19* variations detected in a Japanese population

SNP ID			Refe-rence	Location	Position		Nucleotide change and flanking sequences (5′ to 3′)	Amino acid change	Number of subjects			Frequency		
This Study	JSNP	dbSNP (NCBI)			NT_030059.12	From the translational initiation site or from the end of nearest exon			Wild-type	Hetero-zygote	Homo-zygote	Total (n = 253)	Healthy volunteers (n = 119)	Diabetic patients (n = 134)
MPJ6_2C19_001[a]				Enhancer	15268217	− 2772	GCTCGTGAGGAAG/AAGAGGGTGAACA		230	23	0	0.045	0.055	0.037
MPJ6_2C19_002[a]				Enhancer	15268222_15268229	− 2767_ − 2760	TGAGGAAGAGAGGGTGAACA/-GGTAGAGCACAG		251	2	0	0.004	0.000	0.007
MPJ6_2C19_003[a]				Enhancer	15268269	− 2720	GTAAAGCTATTTT/CATATGATACTAC		230	23	0	0.045	0.055	0.037
MPJ6_2C19_004[a]				Enhancer	15268442	− 2547	GGCTGTGTGTGGG/-TGCAGGGAAAGA		252	1	0	0.002	0.004	0.000
MPJ6_2C19_005[a]				Enhancer	15268444	− 2545	CTGTGTGTGGGTG/TCAGGGAAAGAGG		252	1	0	0.002	0.004	0.000
MPJ6_2C19_006[a]				Enhancer	15268444_15268445	− 2545_ − 2544	CTGTGTGTGGGTGC/-AGGGAAAGAGGC		252	1	0	0.002	0.004	0.000
MPJ6_2C19_007[a]				Enhancer	15268949	− 2040	TAAAGAGAGCAAC/TCAAGCTTATCTT		241	12	0	0.024	0.017	0.030
MPJ6_2C19_008		rs11568732	16)	Promoter	15270100	− 889	CAGAATAACTAAT/GGTTTGGAAGTTG		174	70	9	0.174	0.193	0.157
MPJ6_2C19_009		rs12248560	20)	Promoter	15270183	− 806	CTGTTCTCAAAGC/TATCTCTGATGTA		249	4	0	0.008	0.008	0.007
MPJ6_2C19_010[a]				Promoter	15270211	− 778	GATAATGCGCCAC/TGATGGGCATCAG		252	1	0	0.002	0.000	0.004
MPJ6_2C19_011[a]				Promoter	15270212	− 777	ATAATGCGCCACG/AATGGGCATCAGA		252	1	0	0.002	0.004	0.000
MPJ6_2C19_012[a]				Promoter	15270460	− 529	TTTCATGTTTAGG/CCTGCTGTATTTT		248	5	0	0.010	0.008	0.011
MPJ6_2C19_013[a]				Promoter	15270800	− 189	GACGAAGGAGAAC/AAAGACCAAAGGA		252	1	0	0.002	0.000	0.004
MPJ6_2C19_014[a]				Promoter	15270804	− 185	AAGGAGAACAAGA/GCCAAAGGACATT		252	1	0	0.002	0.000	0.004
MPJ6_2C19_015		rs4986894	16)	Promoter	15270891	− 98	GATTGGCCACTTT/CATCCATCAAAGA		137	97	19	0.267	0.256	0.276
MPJ6_2C19_016		rs17885098	20)	Exon 1	15271087	99	CCCTCCTGGCCCC/TACTCCTCTCCCA	P33P	9	70	174	0.826	0.807	0.843
MPJ6_2C19_017[a]				Exon 1	15271139	151	ATTAAGGATGTCA/GGCAAATCCTTAA	S51G	252	1	0	0.002	0.000	0.004
MPJ6_2C19_018[a]				Intron 1	15271284	IVS1 + 128	TTGAAAGGCTTTT/AGTTGCCTTTTCC		250	3	0	0.006	0.008	0.004
MPJ6_2C19_019		rs17884832		Intron 1	15283001	IVS1 − 340	TTCAAATTTGGGT/GCTTCTGTATATT		174	70	9	0.174	0.193	0.157
MPJ6_2C19_020		rs7916649		Intron 1	15283110	IVS1 − 231	GTTGGTGTGAGGG/ATTAATTGTAATC		76	127	50	0.449	0.458	0.440
MPJ6_2C19_021		rs17878649		Intron 1	15283294	IVS1 − 47	GCTTAGTAAATGG/AACAAAACAGTGA		193	55	5	0.128	0.139	0.119
MPJ6_2C19_022		rs12769205	20)	Intron 2	15283650	IVS2 − 23	GATCTCCCTCCTA/GGTTTCGTTTCTC		137	97	19	0.267	0.256	0.276
MPJ6_2C19_023[a]				Exon 3	15283822	481	AGAAAAACCAAGG/CGTGGGTGAACAT	A161P	250	3	0	0.006	0.000	0.011
MPJ6_2C19_024[a]				Intron 3	15283985	IVS3 + 163	GAATTTGCACATG/ATTTGTGCTGTGT		252	1	0	0.002	0.004	0.000
MPJ6_2C19_025		rs17879992		Intron 3	15284154	IVS3 + 332	TTTTTCCCATTAT/CCTATTCCAGAAC		174	70	9	0.174	0.193	0.157
MPJ6_2C19_026		rs4986893	10)	Exon 4	15288936	636	AAGCACCCCCTGG/AATCCAGGTAAGG	W212X	193	55	5	0.128	0.139	0.119
MPJ6_2C19_027[a]				Intron 4	15289213	IVS4 + 271	TTTCTATAAAGTA/GCTTTGGTGACAG		252	1	0	0.002	0.004	0.000
MPJ6_2C19_028		rs7088784		Intron 4	15289899	IVS4 − 205	GAAATGATTATCA/GTCTTTGATTCTC		174	70	9	0.174	0.193	0.157
MPJ6_2C19_029		rs4244285	9)	Exon 5	15290142	681	TGATTATTTCCCG/AGGAACCCATAAC	splicing defect	137	97	19	0.267	0.256	0.276
MPJ6_2C19_030		rs12571421		Intron 5	15290508	IVS5 + 228	TAAATATAATCTA/GTCTGAACAATAA		137	97	19	0.267	0.256	0.276
MPJ6_2C19_031			20)	Intron 5	15328666	IVS5 − 113	TTTTTCTAGTACT/GATACTTTACAGT		230	23	0	0.045	0.055	0.037
MPJ6_2C19_032		rs4417205	20)	Intron 5	15328728	IVS5 − 51	ATTTACTGTCATC/GAAATATGCTGTT		140	94	19	0.261	0.248	0.272
MPJ6_2C19_033[a]				Intron 5	15328730	IVS5 − 49	TTACTGTCATCAA/GATATGCTGTTAA		252	1	0	0.002	0.000	0.004
MPJ6_2C19_034[a]				Intron 6	15350910	IVS6 − 210	CATATATGTGTAC/TAGATTTTTCTTA		251	2	0	0.004	0.000	0.007
MPJ6_2C19_035[a]				Intron 6	15350924	IVS6 − 196	GATTTTTCTTAAT/AGCCTAGCTTAAG		138	96	19	0.265	0.252	0.276
MPJ6_2C19_036[a]				Intron 6	15351088	IVS6 − 32	CCATTTCTCTCCT/ATTTCCATCAGTT		252	1	0	0.002	0.000	0.004
MPJ6_2C19_037[a]				Exon 7	15351144	986	AAGAGATTGAACG/ATGTCGTTGGCAG	R329H	252	1	0	0.002	0.000	0.004
MPJ6_2C19_038	IMS-JST111900	rs3758580	20)	Exon 7	15351148	990	GATTGAACGTGTC/TGTTGGCAGAAAC	V330V	138	96	19	0.265	0.252	0.276
MPJ6_2C19_039	IMS-JST111901	rs3758581	3)	Exon 7	15351149	991	ATTGAACGTGTCA/GTTGGCAGAAACC	I331V	0	23	230	0.955	0.945	0.963
MPJ6_2C19_040[a]				Exon 7	15351236	1078	CAGAGATACATCG/AACCTCATCCCCA	D360N	252	1	0	0.002	0.000	0.004
MPJ6_2C19_041[a]				Exon 7	15351277	1119	AGTGACCTGTGAC/TGTTAAATTCAGA	D373D	252	1	0	0.002	0.000	0.004
MPJ6_2C19_042[a]				Intron 7	15351391	IVS7 + 84	TCTACCATCACTG/AGGTGAGAGAAGT		252	1	0	0.002	0.004	0.000
MPJ6_2C19_043		rs17882222		Intron 7	15357999	IVS7 − 201	TCCTGATTGTGGG/ACATTTTAGCAAG		241	12	0	0.024	0.017	0.030
MPJ6_2C19_044[a]				Intron 7	15358026	IVS7 − 174	TATTGTCACTGGC/TCTTAAGCTCATG		246	7	0	0.014	0.017	0.030
MPJ6_2C19_045		rs4917623		Intron 7	15358094	IVS7 − 106	TCTTTGGAATGGT/CGTTTCATCATCT		56	126	71	0.530	0.529	0.530
MPJ6_2C19_046		rs17886522	20)	Exon 8	15358301	1251	GGATGAAGGTGGA/CAATTTTAAGAAA	G417G	193	55	5	0.128	0.139	0.119
MPJ6_2C19_047[a]				Intron 8	15358405	IVS8 + 64	GATCAGTTGGAAC/TTTACATGTGCCT		252	1	0	0.002	0.004	0.000
MPJ6_2C19_048		rs12268020		Intron 8	15360897	IVS8 − 119	ATCTACTCATCCC/TTCCTATGATTCA		250	3	0	0.006	0.004	0.007

[a]Novel variations detected in this study.

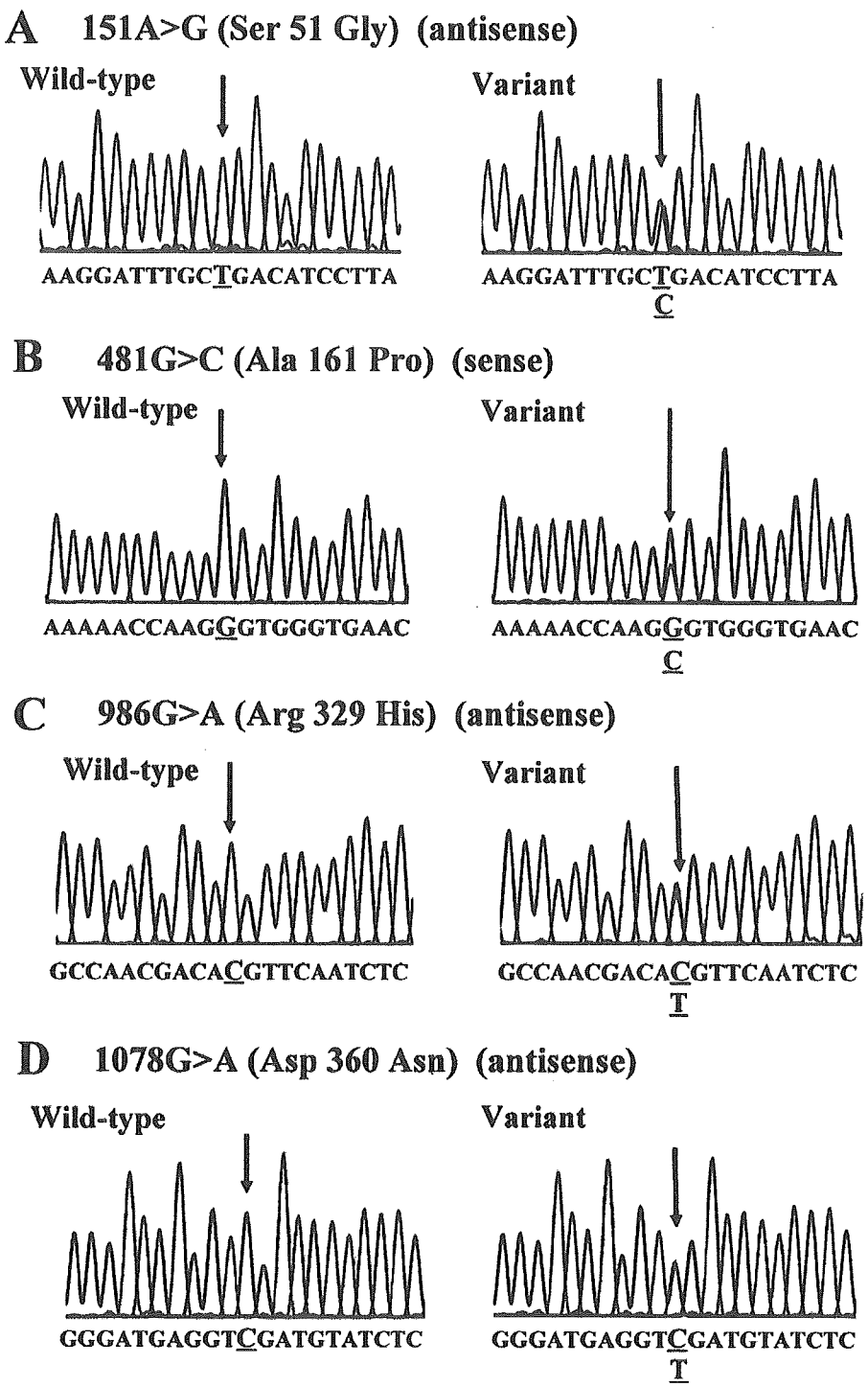

Fig. 1. Four novel nonsynonymous variations of human *CYP2C19*. (A) MPJ6_2C19_017 (wild-type, 151A/A; variant, 151A/G). (B) MPJ6_2C19_023 (wild-type, 481G/G; variant, 481G/C). (C) MPJ6_2C19_037 (wild-type, 986G/G; variant, 986G/A). (D) MPJ6_2C19_040 (wild-type, 1078G/G; variant, 1078G/A). Arrows indicate the positions of the nucleotide changes.

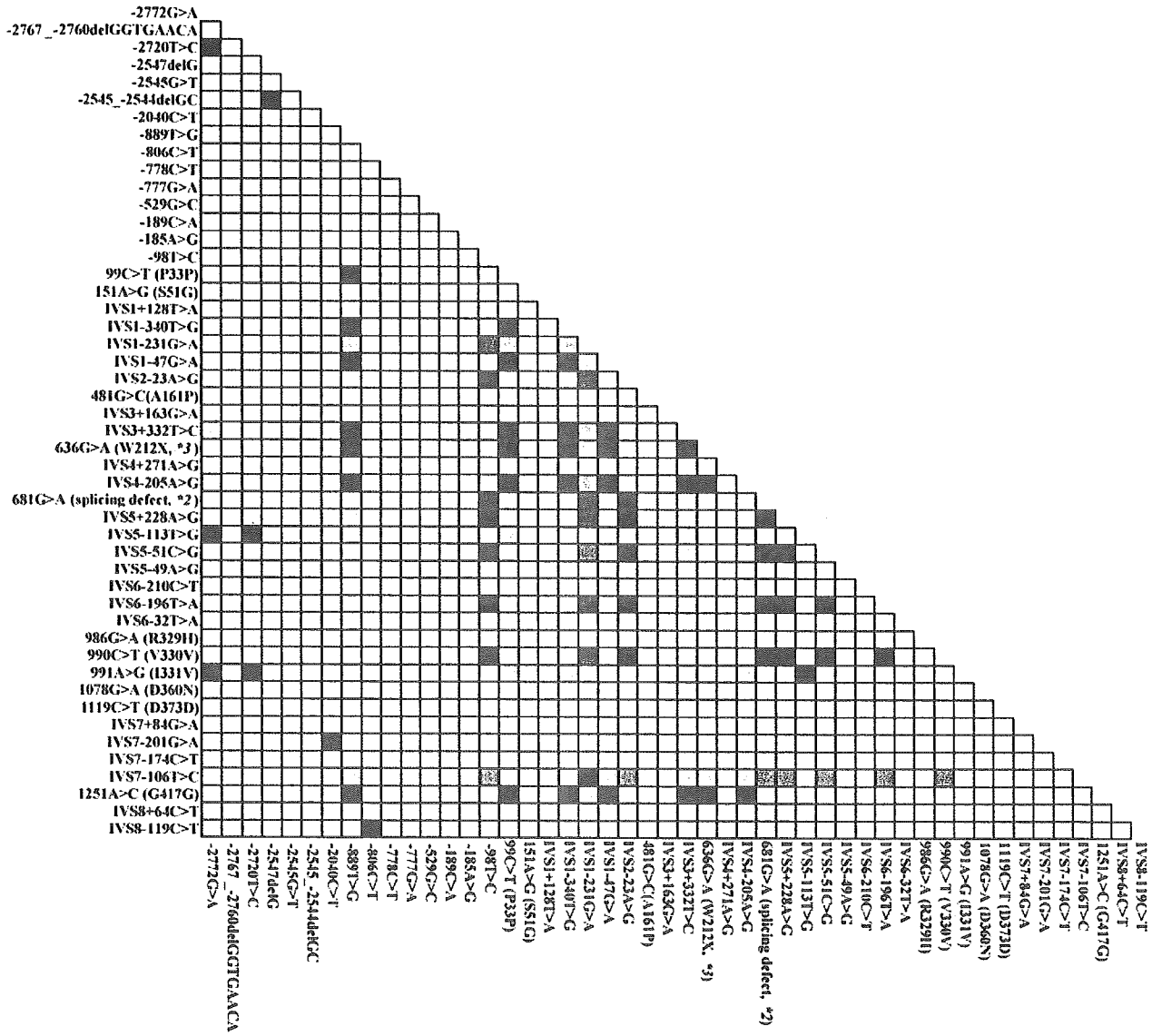

Fig. 2. Linkage disequilibrium (LD) analysis of *CYP2C19* genetic variations.
Pairwise LD is depicted using the r^2 values (from 0 to 1) by a 10-graded gray color. The denser color represents the higher linkage.

conserved in the human CYP2C subfamily.[19] In particular, D360 is located in the substrate recognition site 5.[19] It is possible that the substitution from an acidic (Asp) to a rather neutral (Asn) amino acid might affect the binding of substrates or catalytic activity of the enzyme. The other variations, S51, A161, and R329 are located in the A-helix, in the loop between the D-helix and the E-helix, and in the J-helix, respectively. Further functional analysis should be pursued for these four variations. Moreover, it is necessary to evaluate the real frequencies of the very rare variations found in only one subject (frequency: 0.002).

The two known nonsynonymous SNPs, 681G>A (splicing defect, **2* allele) and 636G>A (W212X; **3* allele) were detected at 0.267 and 0.128 frequencies, respectively. These frequencies were comparable to those of the Japanese in the previous reports.[8,11] The variation 991A>G (I331V, **1B* and **1C* alleles) was found with a 0.955 frequency, indicating that this SNP is rather common in the Japanese population. Other nonsynonymous variations including *CYP2C19*4, *5* and **16* were not detected in this study. Thus, our results confirmed that, except for I331V which has no functional significance, nonsynonymous variations other than *CYP2C19*2* and **3* were very rare in the Japanese population.

Seven and five novel variations were detected in the enhancer and promoter regions, respectively. No variation was found in the reported regions as the binding sites for the constitutive androstane receptor and the glucocorticoid receptor.[17] However, −529G>C was present within the potential negative element (−650 to −453 bases from the translational start site) in the promoter region.[16] Transcriptional activity with this variation needs to be examined in the future.

Using the detected variations, linkage disequilibrium (LD) was analyzed (**Fig. 2**). Perfect linkage ($r^2=1$) was observed among −2772G>A, −2720T>C, IVS5-113T>G, and 991A>G (I331V), between −2547delG and −2545_-2544delGC, and between −2040C>T and IVS7-201G>A. Strong LDs were observed among −98T>C, IVS2-23A>G, 681G>A (splicing defect, **2* allele), IVS5+228A>G, IVS5-51C>G, IVS6-196T>A, and 990C>T (V330V) ($r^2 \geqq 0.96$), between IVS1-231G>A and IVS7-106T>C ($r^2=0.90$), between −806C>T and IVS8-119C>T ($r^2=0.75$), and among −889T>G, 99C>T (P33P), IVS1-340T>G, IVS1-47G>A, IVS3+332T>C, 636G>A (W212X, **3* allele), IVS4-205A>G, and 1251A>C (G417G) ($r^2 \geqq 0.70$). The r^2 values were below 0.45 for the other pairs of variations. Collectively, the LD was observed throughout the *CYP2C19* gene, suggesting that one LD block covers the entire analyzed region spanning approximately 90 kb. Thus, the *CYP2C19* haplotypes were analyzed as one block.

Haplotype analysis was then performed (**Table 3**). The haplotypes registered to the CYP Allele Nomenclature Committee are shown with the numbers (**18* to **21*). The other haplotypes detected in this study are shown as the numbers plus small alphabetical letters. Several haplotypes were first unambiguously assigned by homozygous variations at all sites (**1d*, **2c*, and **3b*) or a heterozygous variation at only one site (**1g*, **1h*, **1k*, **1l*, **1m*, **1n*, and **18*). Separately, the diplotype configuration (a combination of haplotypes) for each subject was estimated by LDSUPPORT software. The additionally inferred haplotypes were six **1* subtype (**1e*, **1f*, **1j*, **1p* to **1r*), eight **2* subtypes (**2d* to **2l*), four **3* subtypes (**3c* to **3f*), **19*, **20*, and **21*. The determined/inferred haplotypes were summarized in **Table 3**. As for **20*, cloning of the amplified genomic DNA and subsequent sequencing confirmed that 1078G>A (D360N) was linked to the **3b* haplotype. The three subjects with heterozygous 481G>C (A161P) had heterozygous 681G>A (**2* allele) concurrently, and the haplotype harboring 481G>C (A161P) was inferred as a subtype of **2c* haplotype (designated as **21*). The most frequent haplotype was **1d* (frequency: 0.492), followed by **2c* (0.241), **3b* (0.115), **1e* (0.043), **1f* (0.022), and **1g* (0.014). The frequencies of the other haplotypes were less than 0.01.

Table 3. Haplotypes of *CYP2C19* in Japanese population

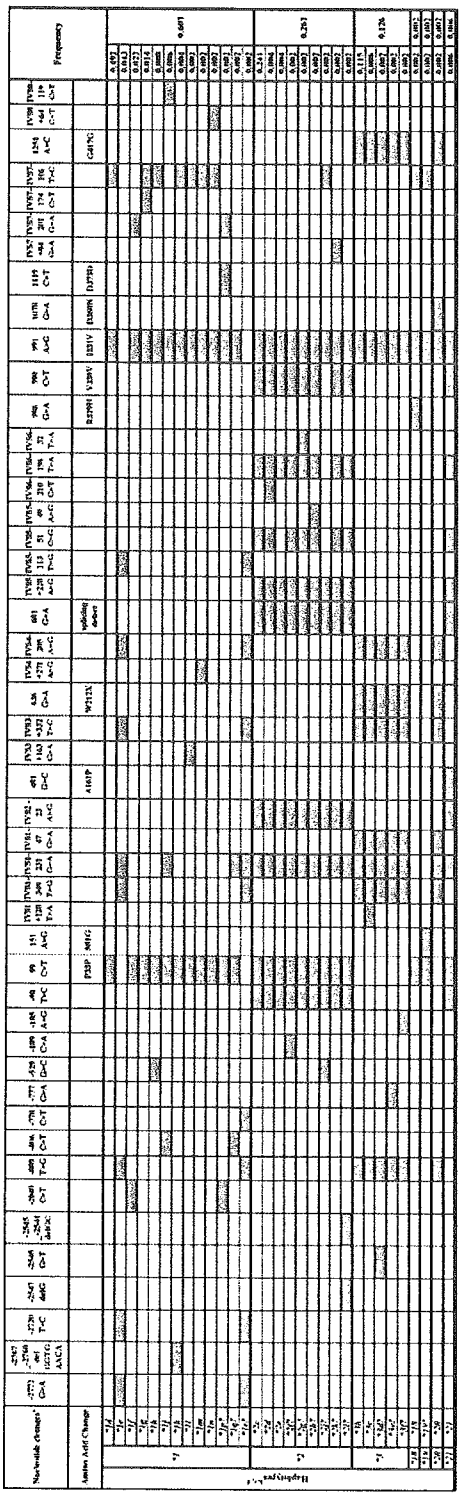

[a]A of the translational start codon of *CYP2C19* is numbered 1. NT_030059.12 was used as the reference sequence.
[b]Major allele, white; minor allele, gray
[c]The haplotypes are described as numbers (plus small alphabetical letters).
[d]The haplotypes inferred in only one subject are described with haplotype names and a question mark.

In conclusion, 48 genetic variations, including 27 novel ones, were detected in *CYP2C19* in a Japanese population. Using the detected variations, 31 haplotypes were determined and/or inferred. Our results would provide fundamental and useful information for genotyping *CYP2C19* in the Japanese and probably other Asian populations.

Acknowledgements: We thank Drs. Yasushi Kaburagi and Sachiko Honjo for aquiring informed consent from the patients, and Ms. Chie Sudo for her secretarial assistance. Hiromi Fukushima-Uesaka and Yoshiro Saito are contributed equally to this work.

References

1) Gray, I. C., Nobile, C., Muresu, R., Ford, S. and Spurr, N. K.: A 2.4-megabase physical map spanning the CYP2C gene cluster on chromosome 10q24. *Genomics* **28**: 328-332 (1995).
2) Goldstein, J. A.: Clinical relevance of genetic polymorphisms in the human CYP2C subfamily. *Br. J. Clin. Pharmacol.* **52**: 349-355 (2001).
3) Richardson, T. H., Jung, F., Griffin, K. J., Wester, M., Raucy, J. L., Kemper, B., Bornheim, L. M., Hassett, C., Omiecinski, C. J. and Johnson, E. F.: A universal approach to the expression of human and rabbit cytochrome P450s of the 2C subfamily in *Escherichia coli*. *Arch. Biochem. Biophys.* **323**: 87-96 (1995).
4) Furuta, T., Ohashi, K., Kobayashi, K., Iida, I., Yoshida, H., Shirai, N., Takashima, M., Kosuge, K., Hanai, H., Chiba, K., Ishizaki, T. and Kaneko, E.: Effects of clarithromycin on the metabolism of omeprazole in relation to *CYP2C19* genotype status in humans. *Clin. Pharmacol. Ther.* **66**: 265-274 (1999).
5) Katsuki, H., Nakamura, C., Arimori, K., Fujiyama, S. and Nakano, M.: Genetic polymorphism of CYP2C19 and lansoprazole pharmacokinetics in Japanese subjects. *Eur. J. Clin. Pharmacol.* **52**: 391-396 (1997).
6) Qin, X. P., Xie, H. G., Wang, W., He, N., Huang, S. L., Xu, Z. H., Ou-Yang, D. S., Wang, Y. J. and Zhou, H. H.: Effect of the gene dosage of *CYP2C19* on diazepam metabolism in Chinese subjects. *Clin. Pharmacol. Ther.* **66**: 642-646 (1999).
7) Furuta, T., Ohashi, K., Kamata, T., Takashima, M., Kosuge, K., Kawasaki, T., Hanai, H., Kubota, T., Ishizaki, T. and Kaneko, E.: Effect of genetic differences in omeprazole metabolism on cure rates for Helicobacter pylori infection and peptic ulcer. *Ann. Intern. Med.* **129**: 1027-1030 (1998).
8) Goldstein, J. A., Ishizaki, T., Chiba, K., de Morais, S. M., Bell, D., Krahn, P. M. and Evans, D. A.: Frequencies of the defective *CYP2C19* alleles responsible for the mephenytoin poor metabolizer phenotype in various Oriental, Caucasian, Saudi Arabian and American black populations. *Pharmacogenetics* **7**: 59-64 (1997).
9) de Morais, S. M., Wilkinson, G. R., Blaisdell, J., Nakamura, K., Meyer, U. A. and Goldstein, J. A.: The major genetic defect responsible for the polymorphism of *S*-mephenytoin metabolism in humans. *J. Biol. Chem.* **269**: 15419-15422 (1994).
10) de Morais, S. M., Wilkinson, G. R., Blaisdell, J., Meyer, U. A., Nakamura, K. and Goldstein, J. A.: Identification of a new genetic defect responsible for the polymorphism of (*S*)-mephenytoin metabolism in Japanese. *Mol. Pharmacol.* **46**: 594-598 (1994).
11) Yamada, S., Onda, M., Kato, S., Matsuda, N., Matsuhisa, T., Yamada, N., Miki, M. and Matsukura, N.: Genetic differences in *CYP2C19* single nucleotide polymorphisms among four Asian populations. *J. Gastroenterol.* **36**: 669-672 (2001).
12) Kubota, T., Chiba, K. and Ishizaki, T.: Genotyping of *S*-mephenytoin 4′-hydroxylation in an extended Japanese population. *Clin. Pharmacol. Ther.* **60**: 661-666 (1996).
13) Morita, J., Kobayashi, K., Wanibuchi, A., Kimura, M., Irie, S., Ishizaki, T. and Chiba, K.: A novel single nucleotide polymorphism (SNP) of the *CYP2C19* gene in a Japanese subject with lowered capacity of mephobarbital 4′-hydroxylation. *Drug Metab. Pharmacokinet.* **19**: 236-238 (2004).
14) Xiao, Z. S., Goldstein, J. A., Xie, H. G., Blaisdell, J., Wang, W., Jiang, C. H., Yan, F. X., He, N., Huang, S. L., Xu, Z. H. and Zhou, H. H.: Differences in the incidence of the *CYP2C19* polymorphism affecting the *S*-mephenytoin phenotype in Chinese Han and Bai populations and identification of a new rare *CYP2C19* mutant allele. *J. Pharmacol. Exp. Ther.* **281**: 604-609 (1997).
15) Garcia-Barcelo, M., Chow, L. Y., Kum Chiu, H. F., Wing, Y. K., Shing Lee, D. T., Lam, K. L. and Waye, M. M.: Frequencies of defective *CYP2C19* alleles in a Hong Kong Chinese population: detection of the rare allele *CYP2C19*4*. *Clin. Chem.* **45**: 2273-2274 (1999).
16) Arefayene, M., Skaar, T. C., Zhao, X., Rae, J. M., Tanus-Santos, J. E., Brinkmann, U., Brehm, I., Salat, U., Nguyen, A., Desta, Z. and Flockhart, D. A.: Sequence diversity and functional characterization of the 5′-regulatory region of human *CYP2C19*. *Pharmacogenetics* **13**: 199-206 (2003).
17) Chen, Y., Ferguson, S. S., Negishi, M. and Goldstein, J. A.: Identification of constitutive androstane receptor and glucocorticoid receptor binding sites in the *CYP2C19* promoter. *Mol. Pharmacol.* **64**: 316-324 (2003).
18) Kitamura, Y., Moriguchi, M., Kaneko, H., Morisaki, H., Morisaki, T., Toyama, K. and Kamatani, N.: Determination of probability distribution of diplotype configuration (diplotype distribution) for each subject from genotypic data using the EM algorithm. *Ann. Hum. Genet.* **66**: 183-193 (2002).
19) Lewis, D. F.: Essential requirements for substrate binding affinity and selectivity toward human CYP2 family enzymes. *Arch. Biochem. Biophys.* **409**: 32-44 (2003).
20) Blaisdell, J., Mohrenweiser, H., Jackson, J., Ferguson, S., Coulter, S., Chanas, B., Xi, T., Ghanayem, B. and Goldstein, J. A.: Identification and functional characterization of new potentially defective alleles of human *CYP2C19*. *Pharmacogenetics* **12**: 703-711 (2002).

Different Effects of Desipramine on Bufuralol 1″-Hydroxylation by Rat and Human CYP2D Enzymes

Takashi ISOBE,[a] Hiroyuki HICHIYA,[a] Nobumitsu HANIOKA,[a] Shigeo YAMAMOTO,[b] Sumio SHINODA,[c] Yoshihiko FUNAE,[d] Tetsuo SATOH,[e] Shigeru YAMANO,[f] and Shizuo NARIMATSU*,[a]

[a] *Laboratory of Health Chemistry, Faculty of Pharmaceutical Sciences, Okayama University;* [b] *Laboratory of Biomolecular Sciences, Faculty of Pharmaceutical Sciences, Okayama University;* [c] *Laboratory of Environmental Hygine, Faculty of Pharmaceutical Sciences, Okayama University; 1–1–1 Tsushima-naka, Okayama 700–8530, Japan:* [d] *Laboratory of Chemistry, Osaka City University Medical School; 1–4–54 Asahimachi, Abeno-ku, Osaka 545–8585, Japan:* [e] *Human Animal Bridge Discussion Group; 2802–1 Hiratsuka, Shiroi, Chiba 270–8601, Japan: and* [f] *Department of Hygienic Chemistry, Faculty of Pharmaceutical Sciences, Fukuoka University; 8–19–1 Nanakuma, Jonan-ku, Fukuoka 814–0180, Japan.* Received November 15, 2004; accepted January 13, 2005

Inhibitory effects of desipramine (DMI) on rat and human CYP2D enzymes were studied using bufuralol (BF) 1″-hydroxylation as an index. Inhibition was examined under the following two conditions: 1) DMI was co-incubated with BF and NADPH in the reaction mixture containing rat or human liver microsomes or yeast cell microsomes expressing rat CYP2D1, CYP2D2 or human CYP2D6 (co-incubation); 2) DMI was preincubated with NADPH and the same enzyme sources prior to adding the substrate (preincubation). When either rat liver microsomes or recombinant CYP2D2 was employed, the preincubation with DMI (0.3 μM) caused a greater inhibition of BF 1″-hydroxylation than the co-incubation did, whereas BF 1″-hydroxylation by rat CYP2D1 was not markedly affected under the same conditions. The inhibitory effect of DMI on BF 1″-hydroxylation by human liver microsomal fractions or recombinant CYP2D6 was much lower than that on the hydroxylation by rat liver microsomes or CYP2D2. Kinetic studies demonstrated that the inhibition-type changed from competitive for the co-incubation to noncompetitive for the preincubation in the case of CYP2D2, whereas the inhibition-type was competitive for both the co-incubation and the preincubation in the case of CYP2D6. Furthermore, the loss of activity of rat CYP2D2 under the preincubation conditions followed pseudo-first-order kinetics. Binding experiments employing the recombinant enzymes and [^{3}H]-DMI revealed that CYP2D2 and CYP2D6 were the only prominent proteins to which considerable radioactive DMI metabolite(s) bound. These results indicate that rat CYP2D2 biotransforms DMI into reactive metabolite(s), which covalently bind to CYP2D2, resulting in inactivation of the enzyme. In contrast, human CYP2D6 may also biotransform DMI into some metabolite(s) that covalently bind to CYP2D6, but that do not inactivate the enzyme.

Key words desipramine; CYP2D2; CYP2D6; reactive metabolite; binding; inactivation

Imipramine (IMI) and desipramine (DMI) are tricyclic antidepressants that are widely used clinically. As shown in Fig. 1, IMI is oxidized by cytochrome P450 (CYP) mainly *via* two pathways: side-chain *N*-demethylation and aromatic ring 2-hydroxylation, forming DMI and 2-hydroxyimipramine (2-OH-IMI), respectively.[1] DMI and 2-OH-IMI further undergo 2-hydroxylation and *N*-demethylation, respectively, forming 2-hydroxy-DMI as the common metabolite (Fig. 1). In the human liver, CYP2D6 is mainly responsible for IMI 2-hydroxylation whereas CYP2C19 and CYP1A2 are involved in *N*-demethylation.[2,3]

It has been reported that repeated administration of IMI to rats changed hepatic CYP-dependent monooxygenase activities.[4—6] We have also found that repetitive oral administration of IMI to rats caused a decrease in hepatic microsomal CYP2D-dependent reactions such as debrisoquine 4-hydroxylation, bunitrolol 4-hydroxylation, lidocaine 3-hydroxylation and propranolol 4-, 5- and 7-hydroxylations.[7] We have proposed that binding of a reactive metabolite of IMI to rat CYP2D enzyme(s) resulted in the decreased enzyme activities.[7] As a possible mechanism, we speculated that an epoxy metabolite of IMI (1,2- or 2,3-epoxide) was involved in the inactivation of rat CYP2D enzyme(s).[7,8]

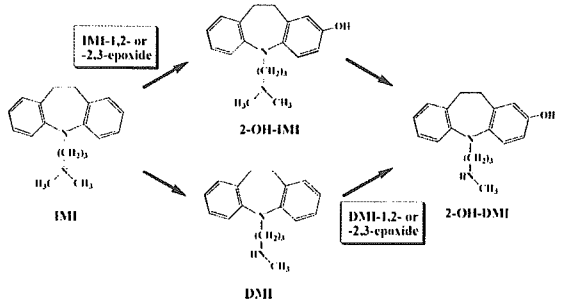

Fig. 1. Parallel Metabolic Pathways of the Conversion of IMI to 2-OH-DMI

If the epoxy metabolite(s) of IMI are responsible for the inactivation, DMI would also inactivate the rat CYP2D enzyme(s). Because several CYP2D enzymes are known to be expressed in the rat liver,[9] it is interesting to know what kind of CYP2D isoenzyme(s) are inhibited by IMI or DMI. Furthermore, there is a possibility that CYP2D6, a human functional CYP2D enzyme, is also inactivated by IMI and DMI in a similar manner. The present study was thus conducted to examine these possibilities using radiolabeled and unlabeled DMI and recombinant human and rat CYP2D enzymes.

MATERIALS AND METHODS

Materials DMI as the hydrochloride and propranolol racemate as the hydrochloride were obtained from Sigma Chemical Co. (St. Louis, MO, U.S.A.); bufuralol (BF) and

* To whom correspondence should be addressed. e-mail: shizuo@pharm.okayama-u.ac.jp

1″-hydroxybufuralol (1″-OH-BF) (both as hydrochlorides) were from Daiichi Pure Chemical Co. (Tokyo, Japan); dithiothreitol was from Nacalai Tesque (Kyoto, Japan); [^{3}H]-labeled DMI (specific activity 2.96 TBq/mmol, radiochemical purity above 97%) was from NEN Life Science Products, Inc. (Boston, MA, U.S.A.); glucose 6-phosphate (G-6-P), G-6-P dehydrogenase and NADPH were from Oriental Yeast Co., Ltd. (Tokyo, Japan). All other chemicals and organic solvents used were of analytical grade.

Rat and Human Liver Microsomes Male Wistar rats (6 weeks old) were purchased from Clea Japan Co. (Shizuoka, Japan). Liver microsomal fractions were prepared from rats by a published method.[10] Human liver microsomal fractions (n=3, all male Caucasians from 25 to 56 years old) were supplied from Human and Animal Bridge Discussion Group (HAB) (Chiba, Japan). This study was approved by the Ethics Committee of the Faculty of Pharmaceutical Sciences, Okayama University.

Recombinant CYP2D Enzymes Recombinant rat CYP2D2[9] and human CYP2D6[11] were expressed in yeast cells (*Saccharomyces cerevisiae* AH-22 strain) according to methods previously reported. Rat CYP2D2-G45V mutant protein, which has valine instead of glycine at position 45 of CYP2D2, was expressed in yeast cells as reported elsewhere.[12] The contents of CYP2D enzymes in yeast cell microsomal fractions were 52.8, 92.0, 2.1 and 6.5 pmol/mg protein for CYP2D6, CYP2D1, CYP2D2 and CYP2D2-G45V, respectively.

Incubation of Rat or Human Liver Microsomal Fractions with IMI or DMI The inhibitory effects of DMI on rat or human liver microsomal BF 1″-hydroxylation were examined under three conditions as summarized in Chart 1a—c: rat or human liver microsomal fraction (0.5 mg protein) was added to ice-cold reaction medium (final volume 500 μl) in a brown glass conical tube (10 ml) with a glass stopper containing 5 mM G-6-P, 1 IU G-6-P dehydrogenase, 5 mM $MgCl_2$, 0.1 mM EDTA, 0.5 mM NADPH in 100 mM potassium phosphate buffer (pH 7.4) and preincubated for 5 min. NADPH (final concentration 0.5 mM) with or without DMI (final concentration 0.3 μM for the rat enzyme sources and 3.0 μM for the human enzyme sources) was added to the equilibrated mixture and allowed to incubate at 37 °C for 2 min, after which BF (final concentration 0.5 μM) was added and BF 1″-hydroxylation was allowed to proceed for 1 min. After the reaction was stopped by adding 1 ml of 1 M NaOH aqueous solution and vortex mixing, 1 ml of 1 M sodium carbonate buffer (pH 9.6) and propranolol racemate (100 nmol, internal standard) were added, and 1″-OH-BF was extracted into 5 ml of ethyl acetate by vigorous shaking. After centrifugation (1000×g for 10 min) 4 ml of the organic layer was taken and evaporated to dryness under N_2 stream. The residue was dissolved in 100 μl of the HPLC mobile phase described below, and an aliquot (10 μl) was subjected to HPLC under the conditions described below. In the case of recombinant enzymes, yeast cell microsomal fractions containing 3 pmol of rat or human recombinant CYP were employed. In preliminary experiments, linearity of product formation as a function of time was confirmed for each case.

HPLC Conditions A Shimadzu LC-9A liquid chromatograph equipped with a Shimadzu RF-10A fluorescence detector, a Rheodyne Model 7125 injector and a Shimadzu C-R4A Chromatopac data processor were used with the following: column, Inertsil ODS (4.6 mm×250 mm, GL Science, Tokyo, Japan); mobile phase, acetonitrile/20 mM perchloric acid (pH 2.5) (35 : 65, by volume) at a flow rate of 1.5 ml/min; detection, fluorescence 252/302 nm (excitation/emission).

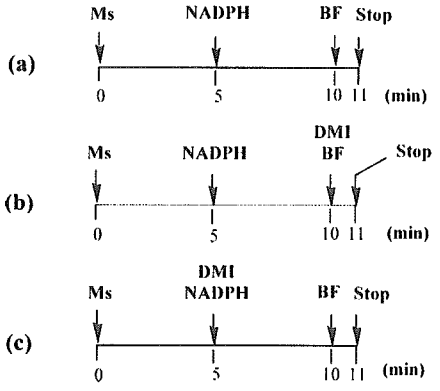

Chart 1

Kinetic Analysis Kinetic studies of BF 1″-hydroxylation by the rat liver microsomes or the recombinant CYP2D enzymes were performed using a BF concentration range from 0.2 to 20 μM and DMI concentration of 0.3 μM for the rat enzymes and 3.0 μM for the human enzyme. Apparent Michaelis constant (K_m) and maximal velocity (V_{max}) were analyzed using the nonlinear least squares regression analysis program MULTI.[13] Inhibition experiments were analyzed by fitting expressions describing competitive inhibition (Eq. 1) and noncompetitive inhibition (Eq. 2) using the same program mentioned above.

$$v = \frac{V_{max} \cdot S}{K_m + (K_m / K_i) \cdot I + S} \quad (1)$$

$$v = \frac{K_i \cdot V_{max} \cdot S}{(K_i + I)(K_m + S)} \quad (2)$$

where v is the rate of formation of metabolite, V_{max} is the maximum rate of metabolite formation, S is the substrate concentration, K_m is the Michaelis constant, I is the inhibitor concentration and K_i is the inhibition constant.

Inactivation of CYP2D2 Microsomes from yeast cells expressing CYP2D2 were preincubated with various concentrations of DMI (0, 0.3, 1.0, 2.0, 5.0 μM) at 37 °C for an appropriate time (0, 0.5, 1, 1.5, 2 min) in the presence of NADPH (0.5 mM). After the preincubation, BF 1″-hydroxylase activities of the preincubated microsomes were assayed as described above. The initial rate constant for the inactivation (K_{obs}) was obtained as slopes of initial linear phase plotting logarithm of remaining activity against the preincubation time. The maximum rate constant for inactivation (K_{inact}) and the dissociation constant for the enzyme-inactivation (K_I) were determined according to the published method.[14]

Binding Studies The yeast cell microsomal fraction expressing CYP2D2 or CYP2D6 (50 pmol) was added to equilibrated incubation mixture containing the same ingredients as described above in the enzyme assay, and preincubated at 37 °C for 5 min. DMI (final concentration 10 μM, 3600000 dpm) was then added, and the mixture was incu-

bated at 37 °C for 30 min in the presence or absence of NADPH (final concentration 0.5 mM). The entire sample mixture was transferred into a dialysis tube, and dialyzed at 4 °C for 6 h against 50 mM Tris–HCl buffer (pH 7.4) containing 20% glycerol, 0.1 mM EDTA and 1 mM dithiothreitol (500 ml×2).

A portion of the dialyzed sample (110 μl) was solubilized and subjected to SDS-PAGE using a 10% slab-gel. The gel was stained with Coomassie Brilliant Blue, and cut into 2-mm strips. The gel strips were then solubilized with hydrogen peroxide, and the radioactivity of the samples was measured using a liquid scintillation counter (LSC-3100, Aloka Co., Tokyo, Japan). The scintillation medium consisted of one volume of Triton X-100 and two volumes of toluene phosphor including 4 g of 2,5-diphenyloxazole and 100 mg of 1,4-bis[2-(4-methyl-5-phenyloxazolyl)] benzene per liter of toluene.

A small portion (10 μl) of the dialyzed sample was subjected to SDS-PAGE using a 10% slab-gel. After electrophoresis, proteins in the gel were transblotted to a PVDF membrane and the CYP2D protein was probed by Western blot analysis using polyclonal antibodies (rabbit IgG) raised against CYP2D1 according to a published method.[15] Various amounts of the recombinant CYP2D enzyme were electrophoresed and transferred to the same membrane, and calibration curves were made by scanning the protein bands corresponding to the CYP2D enzyme using NIH Image (version 1.2) installed in a Power Macintosh G4 equipped with an Epson CC-550L scanner. The localization of the radiolabeled CYP2D enzymes on the PVDF membrane and their radioactivity were measured by imaging analysis with the BAS2000 system (Fuji Film, Co., Tokyo, Japan). The PVDF membrane on which radioactive DMI metabolite(s)-bound proteins were transblotted and another PVDF membrane on which various amounts of [^{3}H]-DMI were spotted were attached to an imaging plate (Fuji Film, Co) and exposed for 2 weeks. Then the imaging plate was scanned using the BAS2000 system, and the radioactivity of the CYP2D2 or CYP2D6 protein band on the membrane was calculated on the basis of the calibration curves.

Others Protein concentrations were determined by the method of Lowry *et al.*[16] Total holo-CYP content was spectrophotometrically measured from reduced carbon monoxide (CO) spectra according to the method of Omura and Sato[10] using 91 $mM^{-1}cm^{-1}$ as an absorption coefficient. Statistical significance was calculated with Student's *t*-test using Prism version 3.0 (Graph Pad Software, San Diego, CA, U.S.A.), and differences were considered to be statistically significant when p was <0.05.

RESULTS

Comparison of Inhibitory Effects of DMI on BF 1″-Hydroxylation by Rat and Human Liver Microsomes and Recombinant CYP Enzymes In our previous report, we proposed that rat liver microsomal CYP2D enzyme(s) might be inactivated by reactive intermediate(s) formed during IMI metabolism.[8] We thought similarly that CYP2D2 might be a target enzyme that is inactivated during the metabolism of DMI in rat liver microsomes. As the first stage of the present study to test this possibility, we thus compared the inhibitory effects of DMI on BF 1″-hydroxylation between rat liver microsomes (Fig. 2A) and yeast cell microsomes expressing CYP2D1 (Fig. 2B) or CYP2D2 (Fig. 2C) using a DMI concentration of 0.3 μM and a BF concentration of 0.5 μM.

These concentrations of the inhibitor and substrate were chosen to distinguish the inhibition-types of DMI for BF 1″-hydroxylation as clearly as possible, because preliminary

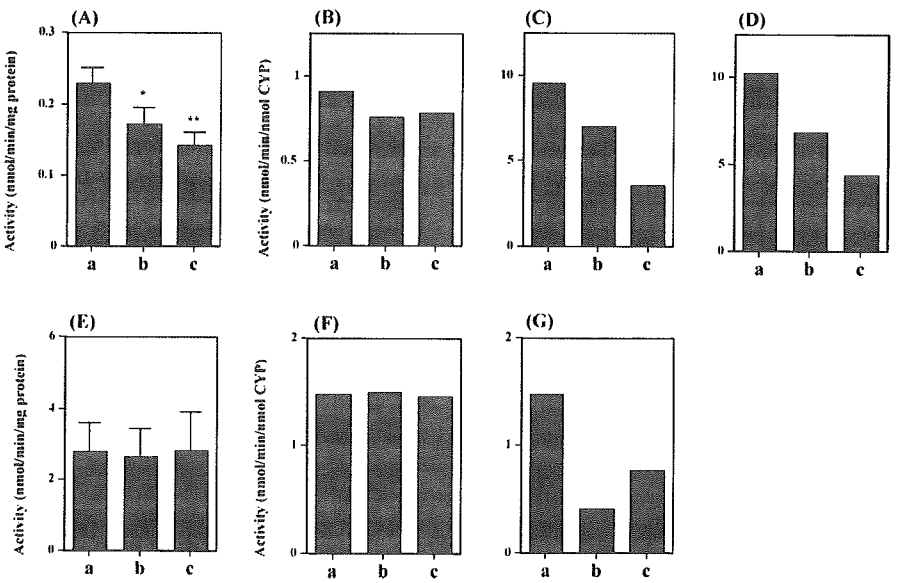

Fig. 2. Comparison of the Inhibitory Effects of DMI on BF 1″-Hydroxylation by Rat or Human Liver Microsomes or Yeast Cell Microsomes Expressing Recombinant CYP Enzymes

The reaction mixtures (final 500 μl) containing various enzyme sources were incubated with BF (0.5 μM) in the presence or absence of DMI (0.3 μM) under the conditions given in Charts 1a, b and c. The enzyme sources were; (A) rat liver microsomes, (B) yeast cell microsomes expressing rat CYP2D2, (C) yeast cell microsomes expressing rat CYP2D2-G45V, (D) human liver microsomes, (E) and (F) yeast cell microsomes expressing human CYP2D6. The concentration of DMI was 0.3 μM except in (F) (3.0 μM). Each value in (A) and (E) is the mean ± S.D. (n=3). Each value in (B), (C), (D), (F) and (G) is the mean value of two independent determinations. Significantly different from the control (a): $*p<0.05$, $**p<0.01$.

studies indicated that most of 0.3 μM DMI disappeared from the reaction mixture during a 2 min incubation and at least 50% of 0.5 μM BF remained after a 1 min incubation under the conditions employed. The co-incubation of BF with DMI significantly inhibited rat hepatic microsomal BF 1″-hydroxylation (Fig. 2A-b) and the preincubation of microsomes with DMI in the presence of NADPH caused a greater inhibition (Fig. 2A-c).

When the recombinant CYP2D1 was used as enzyme source, DMI did not exhibit any clear inhibitory effect on BF 1″-hydroxylase activity (Fig. 2B). On the other hand, DMI produced a greater inhibition of BF 1″-hydroxylation by recombinant CYP2D2 (Fig. 2C). The preincubation of DMI with yeast cell microsomes expressing CYP2D2 in the presence of the cofactor suppressed the activity to 37% of the control level (Fig. 2C-c).

It has been reported that three CYP2D enzymes (CYP2D1, CYP2D2 and CYP2D3) are expressed in the rat liver, and that the microsomal contents of functional CYP2D2 are much lower than those of CYP2D1 and CYP2D3.[17] We recently found that the difference of amino acid residues at positions 43 (tryptophan for CYP2D1 and leucine for CYP2D2) and 45 (valine for CYP2D1 and glycine for CYP2D2) within or near the proline-rich region of the N-terminal region causes the difference in the microsomal functional P450 contents between CYP2D1 and CYP2D2.[12] In that study, we prepared recombinant CYP2D2-G45V having valine instead of glycine-45 and found that the yeast cell microsomal content of the functional holoprotein, P450, was 2- to 3-fold that of wild-type CYP2D2.[12] In the present study, DMI showed a similar inhibition profile for BF 1″-hydroxylation by the wild-type CYP2D2 (Fig. 2C) and by the mutant CYP2D2 (Fig. 2D). Therefore, the inhibitory properties of DMI for CYP2D2 and CYP2D2-G45V are thought to be essentially the same. On the basis of these results, CYP2D2-G45V was used as CYP2D2 in further experiments.

The inhibitory properties of DMI were also examined for human liver microsomes (Fig. 2E) and for yeast cell microsomes expressing recombinant human CYP2D6 (Figs. 2F, G). Interestingly, DMI (0.3 μM) did not cause any inhibitory effect on BF 1″-hydroxylation by either the human liver microsomes (Fig. 2E) or the recombinant CYP2D6 (Fig. 2F). When a 10-times higher concentration of DMI (3 μM) was employed, a considerable inhibition was observed (Fig. 2G). These results indicate that the inhibitory effect of DMI on BF 1″-hydroxylation is much stronger with CYP2D2 than with CYP2D1 and CYP2D6.

Kinetic Studies of the Inhibition by DMI of BF 1″-Hydroxylation by Rat and Human Liver Microsomes and by the Recombinant CYP2D Enzymes Figure 3 shows typical Lineweaver-Burk plots for the inhibition of BF 1″-hydroxylation by rat liver microsomes (A), CYP2D2 (B) and CYP2D6 (C). In plots in (A) and (B), the co-incubation of DMI and BF yielded a competitive-type inhibition, whereas the preincubation of DMI with rat liver microsomes and CYP2D2 in the presence of NADPH changed the inhibition-type from competitive to noncompetitive. The calculated kinetic parameters are summarized in Table 1.

These results demonstrate that BF 1″-hydroxylation was inhibited competitively when rat CYP2D2 was co-incubated with DMI and BF in the presence of NADPH (Chart 1b) and noncompetitively when the enzyme was preincubated with DMI and NADPH before the incubation with BF (Chart 1c). The K_i value for the recombinant CYP2D2 was 0.3 μM, which was lower than that (0.6 μM) for the rat liver microsomes. It is possible that the rat liver microsomes contain not

Table 1. Kinetic Parameters of BF 1″-Hydroxylation by Microsomal Fractions from Rat Livers and Yeast Cells Expressing Rat CYP2D2 or Human CYP2D6

	K_m (μM)	V_{max} [a]	K_i (μM)
Rat liver microsomes			
(A) Control	1.6	2.73	—
(B) Co-incubation[b]	2.3	2.66	0.62
(C) Preincubation[c]	1.7	1.81	0.58
Recombinant CYP2D2			
(A) Control	0.9	94.3	—
(B) Co-incubation[b]	1.7	95.8	0.33
(C) Preincubation[c]	0.9	42.5	0.25
Recombinant CYP2D6			
(A) Control	3.6	16.7	—
(B) Co-incubation[b]	10.3	14.9	1.61
(C) Preincubation[c]	9.8	15.9	1.74

a) nmol/min/mg protein for rat liver microsomes; nmol/min/nmol CYP for recombinant enzymes. *b*) DMI (0.3 μM for the rat-derived enzymes; 3 μM for CYP2D6) together with BF (0.2 to 20 μM) was added to the equilibrated mixture and the mixture was incubated for 1 min. *c*) DMI (0.3 μM for the rat-derived enzymes; 3 μM for CYP2D6) was preincubated with the microsomal fraction in the presence of NADPH (0.5 M) at 37 °C for 2 min, followed by incubation with BF (0.2 to 20 μM) for 1 min. Each value is the mean of two independent determinations.

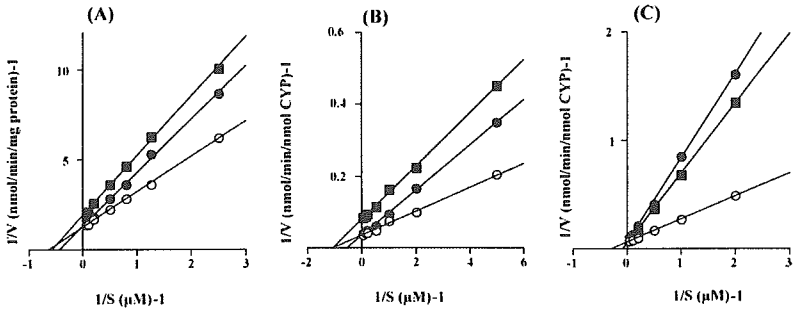

Fig. 3. Lineweaver-Burk Plots Showing the Inhibitory Effects of DMI on BF 1″-Hydroxyation by Rat Liver Microsomes and Yeast Cell Microsomes Expressing Rat CYP2D2 or Human CYP2D6

In the cases of rat liver microsomes (A) and CYP2D2 (B), DMI (0.3 μM) was used. In the case of human CYP2D6 (C), DMI (3.0 μM) was employed. Open circles, control; closed circles, co-incubation; closed squares, preincubation. The protocols for the co-incubation and preincubation are described in Chart 1. Each value represents the mean of duplicate determinations.

only CYP2D2 but also other enzyme(s) that function as BF 1″-hydroxylase and that are relatively resistant to the inactivation by DMI.

In the plots in Fig. 3C using human CYP2D6, on the other hand, the inhibition type was the same, *i.e.*, competitive inhibition, for both co-incubation and preincubation. Furthermore, the K_i value calculated for the human recombinant enzyme was 1.7 μM, which was 5 to 6 times higher than that for the rat recombinant enzyme. This result supports the results in Fig. 2 showing that the inhibitory effect of DMI was much higher for BF 1″-hydroxylation by CYP2D2 than for that by CYP2D6.

Inactivation of CYP2D2 by DMI In order to further characterize the inactivation of CYP2D2 by DMI, the recombinant enzyme was preincubated with various concentrations of DMI in the presence of NADPH, and remaining enzyme activities were assayed. As shown in Fig. 4A, pseudo-first order kinetics were observed for the initial phase of the inactivation. Double reciprocal plots of the rate of inactivation of BF 1″-hydroxylase activity as a function of DMI concetration yielded K_{inact} and K_I values to be 0.19 min^{-1} and 0.76 μM, respectively (Fig. 4B).

Binding of DMI Metabolite(s) to CYP2D Enzymes [^{3}H]-DMI (10 μM, 3600000 dpm) was incubated with yeast cell microsomal fractions expressing CYP2D2 or CYP2D6 (50 pmol) in the presence of an NADPH-generating system. After the incubation, a portion of the reaction mixture was subjected to SDS-PAGE. Proteins in the gels were transblotted to a PVDF membrane and were analyzed by Western blotting using polyclonal antibodies (rabbit IgG) raised against CYP2D1. In Fig. 5, the upper panels A and B are for CYP2D2 and the lower panels C and D for CYP2D6. In the Western blot analysis of CYP2D2 incubated with radioactive DMI (Fig. 5 panel A-b), there was only one protein band whose molecular weight was 51 kDa on the PVDF membrane. Imaging analysis of the membrane using the BAS2000 system showed that the 51 kDa protein was the only protein band with considerable radioactivity (Fig. 5, panel A-c).

The localization of radioactivity was also confirmed by cutting the slab gel after SDS-PAGE and measuring the radioactivity in the gel strips by liquid scintillation counting. As depicted in Fig. 5 panel B, there was a prominent radioactive peak whose location coincided with that of CYP2D2. On

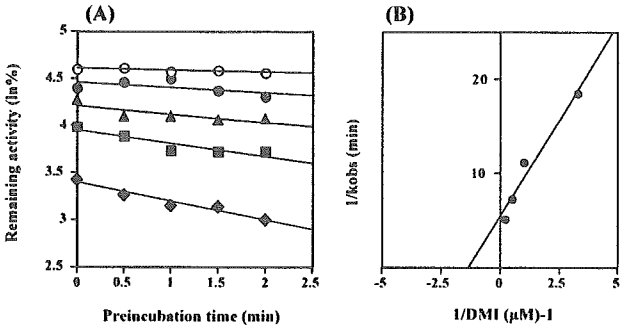

Fig. 4. Time- and Concentration-Dependent Loss of BF 1″-Hydroxylase Activity of CYP2D2 by Preincubation with DMI (A)

Incubation conditions were described under Materials and Methods. The concentrations of DMI were: open circles 0; closed circles 0.3 μM; closed triangles 1 μM; closed squares 2 μM; closed diamonds 5 μM. The reciprocal of first-order inactivation constants obtained from (A) and that of DMI concentrations were plotted (B), yielding the maximal rate of the inactivation (K_{inact}, 0.19 min^{-1}) and the inhibitor concentration required for the half-maximal rate of inactivation (K_I, 0.76 μM).

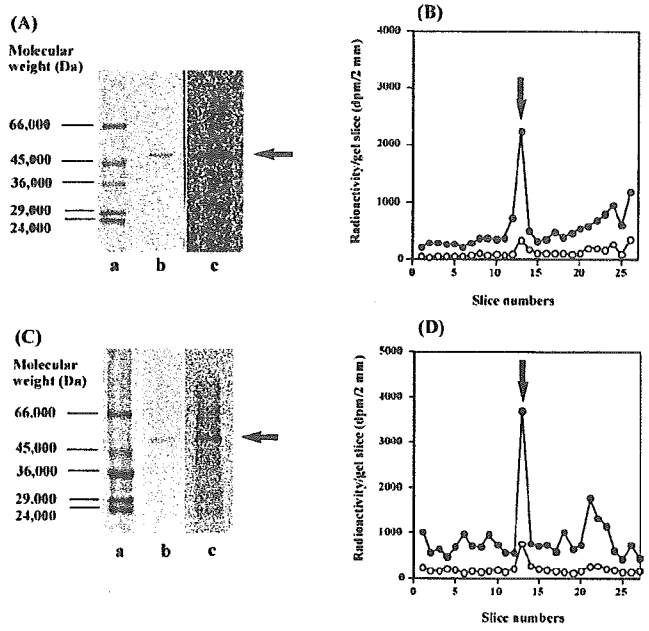

Fig. 5. Detection of Radioactive DMI Metabolite(s)-Bound Proteins by Western Blotting, BAS2000 Imaging Analysis and SDS-PAGE

The yeast cell microsomal fraction expressing rat CYP2D2 or human CYP2D6 (50 pmol each) was incubated with DMI under the conditions described in Materials and Methods. A part of the reaction medium was subjected to SDS-PAGE, and proteins in the gel were transblotted to a PVDF membrane. Proteins and their radioactivities were analyzed by Western blotting and using a BAS2000 image analyzer, respectively (left panels). Another part of the reaction medium was subjected to SDS-PAGE using a 10% slab-gel. The gel was cut into slices of 2 mm each, and their radioactivity was measured by liquid scintillation counting (right panels). Upper panels, rat CYP2D2; lower panels, human CYP2D6. The left panels: a, molecular weight markers; b, a PVDF membrane on which radiolabeled proteins were transblotted was analyzed by Western blotting; c, a scanning image of the PVDF membrane obtained using the BAS2000 imaging analyzer. The arrow shows the CYP2D proteins. The right panels: the sample was incubated in the presence (closed circles) or absence (open circles) of NADPH. Molecular weight markers; bovine albumin 66000; egg albumin, 45000; rabbit muscle glyceraldehyde 3-phosphate dehydrogenase, 36000; bovine carbonic anhydrase, 29000; bovine pancreas trypsinogen, 24000.

the basis of the radioactivity in the gel strip where CYP2D2 was localized, 33 pmol of radioactive metabolite(s) derived from DMI were calculated to bind to 50 pmol of CYP2D2. This means that DMI metabolite(s) were bound to about 70% of the enzyme during the incubation assuming that the binding mol ratio of the enzyme to the metabolite is 1. Results from the imaging analysis using the BAS2000 system also supported these conclusions (data not shown).

The results of binding experiments using human CYP2D6 were similar to those using rat CYP2D2 described above. In this case, 46 pmol of radioactive metabolite(s) derived from DMI were calculated to bind to 50 pmol of CYP2D6. However, in addition to the major peak of CYP2D6 protein, some radioactive peaks with molecular weights smaller than that of CYP2D6 were observed in Fig. 5 panel D, although they were not very prominent. BAS2000 imaging analysis also gave similar results (Fig. 5 panel C-c).

DISCCUSSION

Our previous studies suggested that rat hepatic microsomal CYP2D enzyme(s) were inactivated by IMI during its oxidative metabolism.[8] In the present study, we confirmed that DMI also inhibited BF 1″-hydroxylation by recombinant CYP2D2 as well as by rat liver microsomes. However, CYP2D1, another major CYP2D enzyme in the rat liver, was not markedly affected by DMI under the conditions used.

Interestingly, BF 1″-hydroxylation by human liver microsomes was not affected by DMI at 0.3 μM, which efficiently inhibited the same reaction by rat liver microsomes and recombinant CYP2D2. The human liver microsmal preparations (n=3) used in this study were examined for their CYP2D6 contents (17.6±6.4 pmol/mg protein) and debrisoquine 4-hydroxylase activities (39.6±14.6 nmol/min/mg protein) prior to starting the present study. These results indicate that the functions of CYP2D6 in the human liver microsomal fractions used in the present study were within normal levels. Our finding that BF 1″-hydroxylation by recombinant CYP2D6 was not inhibited by DMI at 0.3 μM but was inhibited at 3.0 μM also suggests that the sensitivity of human CYP2D6 to DMI is lower than that of rat CYP2D2. The difference in the inhibition constants (0.3 μM for CYP2D2 and 1.7 μM for CYP2D6) well supports this notion.

In BF 1″-hydroxylation by the rat enzyme, the inhibition-type of DMI was found to change from competitive under the co-incubation conditions to noncompetitive under the preincubation conditions. To further characterize the inhibition properties, CYP2D2 was preincubated for 0.5 to 2 min with various concentrations of DMI in the presence of NADPH, followed by the assay of BF 1″-hydroxylase activity. The loss of the activity was found to be kinetically pseudo-first-order and saturable, indicating that DMI is a mechanism-based inhibitor for BF 1″-hydroxylation by CYP2D2.

From the profile of the change in the enzyme activity following co-incubation (Fig. 2b) and preincubation (Fig. 2c), the activity of the preincubated microsomes from yeast cell expressing CYP2D2 tends to be lower than that of the co-incubated microsomes (Figs. 2B, C). It is reasonable to think that competitive inhibition is responsible for the decreased activity in the co-incubation, whereas mechanism-based inactivation is mainly responsible for the decreased activity in the preincubation. In contrast, the activity of preincubated microsomes expressing CYP2D6 is higher than that of co-incubated microsomes. This result suggests that in this case, mechanism-based inactivation does not occur or if occurs, to much lesser extent as compared to the case of CYP2D2, and competitive inhibition is mainly responsible for the decreased activity of co-incubated and preincubated microsomes. The phenomenon that the activity of the preincubated microsomes was higher than that of the co-incubated microsomes may be due to the consumption to some extent of DMI during the preincubation with microsomes and the cofactor.

In another experiment using human CYP2D6, preincubation time was prolonged from 2 min to 4 or 6 min, yielding similar results in which the activities in the case of preincubation were higher than those in the case of co-incubation (data not shown). Therefore, it is feasible that, compared to rat CYP2D2, human CYP2D6 is resistant to the inactivation by DMI.

The binding study demonstrated that radioactivity derived from [^{3}H]-DMI bound to CYP2D2. Taking the results of the binding study into account, it is reasonable to think that some reactive metabolite(s) might be formed by CYP2D2 during the preincubation and bind to the enzyme, probably to an amino aid residue which is located in the active site of the enzyme, resulting in the inactivation of the enzyme.

It is noteworthy that in contrast to the results obtained with the rat enzyme, the human enzyme was not inactivated by preincubation with DMI and NADPH, though considerable radioactivity derived from [^{3}H]-DMI was shown to bind to the human enzyme. It is possible that, similarly to the case of the rat CYP2D2, some reactive metabolite(s) are formed from DMI by human CYP2D6 and bind to the enzyme. In this case, however, the binding of the metabolite(s) may not affect the function of the enzyme. It is unclear at present what species of reactive metabolite(s) of DMI and what amino acid residues of the enzymes are involved in the binding described above. Further studies proceeding in this laboratory will clarify these points in the near future.

In summary, the inhibitory effects of DMI on rat and human CYP2D enzymes were studied using BF 1″-hydroxylation as an index. BF 1″-hydroxylation was inhibited competitively when rat CYP2D2 was co-incubated with DMI and BF in the presence of NADPH and noncompetitively when the enzyme was preincubated with DMI and NADPH before the incubation with BF, whereas BF 1″-hydroxylation by rat CYP2D1 was not markedly affected under the same conditions. In contrast, BF 1″-hydroxylation by human liver microsomes and recombinant CYP2D6 was competitively inhibited by DMI in both the co-incubation and the preincubation. The loss of activity of rat CYP2D2 under the preincubation conditions followed pseudo-first-order kinetics. Binding experiments using the recombinant CYP2D enzymes revealed that CYP2D2 and CYP2D6 were the only prominent proteins to which considerable radioactive DMI metabolite(s) bound. These results indicate that DMI was metabolized by the CYP2D enzymes to reactive metabolite(s), which bind to CYP2D proteins, resulting in the inactivation of rat CYP2D2 but not human CYP2D6.

REFERENCES

1) Sallee F. R., Pollock B. G., *Clin. Pharmacokinet.*, **18**, 346—364 (1990).
2) Koyama E., Chiba K., Tani M., Ishizaki T., *J. Pharmacol. Exp. Ther.*, **281**, 1199—1210 (1997).
3) Madsen H., Rasmussen B., Brosen K., *Clin. Pharmacol. Ther.*, **61**, 319—324 (1997).
4) Breyer U., *Naunyn-Schmiedebergs Arch. Pharmacol.*, **272**, 277—288 (1972).
5) Daniel W., Friebertshauser J., Steffen C., *Naunyn-Schmiedebergs Arch. Pharmacol.*, **328**, 83—86 (1984).
6) Daniel W., Netter J., *Naunyn-Schmiedebergs Arch. Pharmacol.*, **342**, 234—240 (1990).
7) Masubuchi Y., Takahashi C., Fujio N., Horie T., Suzuki T., Imaoka S., Funae Y., Narimatsu S., *Drug Metab. Dispos.*, **23**, 999—1003 (1995).
8) Masubuchi Y., Igarashi S., Suzuki T., Horie T., Narimatsu S., *J. Pharmacol. Exp. Ther.*, **279**, 724—731 (1996).
9) Wan J., Imaoka S., Chow T., Hiroi T., Yabusaki Y., Funae Y., *Arch. Biochem. Biophys.*, **348**, 383—390 (1997).
10) Omura T., Sato R., *J. Biol. Chem.*, **239**, 2370—2378 (1964).
11) Tsuzuki D., Takemi C., Yamamoto S., Tamagake K., Imaoka S., Funae Y., Kataoka H., Shinoda S., Narimatsu S., *Pharmacogenetics*, **11**, 709—718 (2001).
12) Narimatsu S., Imoto K., Isobe T., Kiryu K., Naito S., Hichiya H., Funae Y., Hanioka N., Yamamoto S., *Biochem. Biophys. Res. Commun.*, **324**, 627—633 (2004).
13) Yamaoka K., Tanigawara Y., Nakagawa T., Uno T., *J. Pharmacobio-Dyn.*, **4**, 879—885 (1981).
14) Silverman R. B., "Chemistry and Enzymology," Vol. 1, CRC Press, Boca Raton, FL, 1988, pp. 3—30.
15) Guengerich F. P., Wang P., Davidson N. K., *Biochemistry*, **21**, 1698—1706 (1982).
16) Lowry O. H., Rosebrough N. J., Farr A. L., Randall R. J., *J. Biol. Chem.*, **193**, 265—275 (1951).
17) Hiroi T., Imaoka S., Chow T., Funae Y., *Biochim. Biophys. Acta*, **1380**, 305—312 (1998).

Available online at www.sciencedirect.com
SCIENCE DIRECT®
Chemico-Biological Interactions 159 (2006) 47–57
Chemico-Biological Interactions
www.elsevier.com/locate/chembioint

The effect of dimethyl sulfoxide on the function of cytochrome P450 2D6 in HepG2 cells upon the co-expression with NADPH-cytochrome P450 reductase

Shizuo Narimatsu [a,*], Noriko Takatsu [b], Shigeru Yamano [c], Yusuke Inoue [d], Nobumitsu Hanioka [a], Kimio Kiryu [e], Shinsaku Naito [e], Frank J. Gonzalez [f], Shigeo Yamamoto [b]

[a] *Laboratory of Health Chemistry, Graduate School of Medicine, Dentistry and Pharmaceutical Sciences, Okayama University, 1-1-1 Tsushima-naka, Okayama 700-8530, Japan*
[b] *Laboratory of Biomolecular Sciences, Graduate School of Medicine, Dentistry and Pharmaceutical Sciences, Okayama University, Okayama 700-8530, Japan*
[c] *Department of Hygienic Chemistry, Faculty of Pharmaceutical Sciences, Fukuoka University, Jonan-ku, Fukuoka 814-0180, Japan*
[d] *Department of Biological and Chemical Engineering, Faculty of Engineering, Gunma University, Kiryu, Gunma 376-8515, Japan*
[e] *Division of Pharmacology, Drug Safety and Metabolism, Otsuka Pharmaceutical Factory Inc., Naruto, Tokushima 772-8601, Japan*
[f] *National Cancer Institute, National Institutes of Health, Bethesda, MD 20892, USA*

Received 10 August 2005; received in revised form 2 September 2005; accepted 2 September 2005
Available online 7 October 2005

Abstract

HepG2 cells, a human hepatoma cell line, stably expressing NADPH-cytochrome P450 reductase (OR) and/or cytochrome P450 2D6 wild-type (CYP2D6-WT) or its variants (Pro34Ser, Gly42Arg, Arg296Cys and Ser486Thr) were established in the present study. The cultivation of HepG2 cells expressing CYP2D6-WT in the culture medium containing dimethyl sulfoxide (DMSO, 0.1% of final concentration) markedly increased the bufuralol (BF) 1″-hydroxylase activity compared with that of control cells when cultivated without DMSO. A similar effect was also observed in HepG2 cells stably expressing CYP2D6 and OR. The addition of hemin in place of DMSO to the culture medium resulted in no increase in the enzyme activity. Western blot analysis revealed that the levels of CYP2D6 protein were similar between DMSO-treated and non-treated HepG2 cells regardless of OR expression. Spectrophotometric analysis of reduced carbon monoxide-difference spectra of HepG2 cells expressing CYP2D6-WT and/or OR demonstrated that the addition of DMSO increased the peak height of functional CYP2D6 at 450 nm. These results suggest that the increase in CYP2D6 activity is attributable to the radical-scavenging effect of DMSO. The HepG2 cell lines stably expressing OR and CYP2D6 or its variants in combination with DMSO treatment may be useful for screening the cytotoxicity of chemical compounds which undergo oxidation by CYP2D6.

Keywords: CYP2D6; HepG2 cell line; NADPH-cytochrome P450 reductase; Dimethyl sulfoxide; Bufuralol

Abbreviations: CYP, cytochrome P450; OR, NADPH-cytochrome P450 reductase; DMSO, dimethyl sulfoxide; BF, bufuralol; CO, carbon monoxide; CHO, Chinese hamster ovary; PVDF, polyvinylidene difluoride

* Corresponding author. Tel.: +81 86 251 7942; fax: +81 86 251 7942.
E-mail address: shizuo@pharm.okayama-u.ac.jp (S. Narimatsu).

0009-2797/$ – see front matter © 2005 Elsevier Ireland Ltd. All rights reserved.
doi:10.1016/j.cbi.2005.09.001

1. Introduction

Cytochrome P450 2D6 (CYP2D6) is an important drug-metabolizing CYP enzyme. This enzyme constitutes at most 2% of the total CYP contents of the human liver, but is responsible for the major metabolic pathways of over 70 medicines that are often prescribed clinically [1–3]. Furthermore, it is well known that this CYP enzyme shows extensive genetic polymorphism, and 7 to 10% of the Caucasian population is deficient in the CYP2D6 enzymatic function, whereas 1% or less of the Asian population, including the Japanese population, is deficient [4].

It has been reported that a single nucleotide polymorphism occurs at nucleotide position 118 of the CYP2D6 cDNA resulting in the amino acid substitution of proline to serine at position 34, which was found in CYP2D6*4, CYP2D6*10 and CYP2D6*14 [4]. This substitution (P34S) which significantly interferes with the enzymatic functions is present in approximately 30% of the Japanese population. Our previous findings indicate that the P34S substitution causes dysfunction in the anchoring N-terminal region of CYP2D6 in membranes of the endoplasmic reticulum [5].

Various amino acid substitutions, including P34S, have been reported to occur in the CYP2D6 protein, and the influence of some substitutions on enzymatic functions has been evaluated using typical substrates [4,6]. Moreover, it seems possible that the substitutions of amino acid residues modify the enzymatic functions of CYP2D6, resulting in undesired toxicity due to the formation of novel metabolites from medicines as substrates. We can examine this possibility if appropriate human cell systems co-expressing NADPH-CYP reductase (OR) and CYP enzyme or its mutants are available.

We previously established a yeast cell system transfected with cDNA encoding CYP2D6 or its various variants [5,7,8]. However, we thought that the yeast cell system might be inadequate for the assay of cytotoxicity for human cells. Therefore here, we established a human hepatoma cell line, HepG2 cells, stably expressing human OR as the first step, and then expressed or its various variants in these cells to examine their enzymatic functions.

2. Materials and methods

2.1. Materials

BF racemate and 1″-hydroxybufuralol (as hydrochlorides) were obtained from Daiichi Chemical Co. (Tokyo, Japan). Dimethyl sulfoxide (DMSO) and hemin were purchased from Nacalai Tesque (Kyoto, Japan); cytochrome *c* (from horse heart, type V) was from Sigma Chemicals Co. (St. Louis, MO); HepG2 cells were from Riken BioResource Center (Ibaraki, Japan). Human OR cDNA cloned into pGEM-3Z was supplied by Dr. J. Goldstein (NIEHS, Research Triangle Park, NC).

2.2. Construction of expression plasmids

For the expression of human OR in HepG2 cells, the *Eco*RI–*Xba*I fragment which was ligated into pTracer-EF A (Invitrogen, Carlsbad, CA) was prepared using pGEM-3Z as the template with a forward primer (5′-CGGAATTCAAAATGGGAGACTCCA-CGTGGACAC-3′, the *Eco*RI site and a Kozak sequence are marked with a solid line and a broken line, respectively), and a reverse primer (5′-TGCTCTAGA-GTGGGTGGGGCAGGCAGGTTTT-TAG-3′, the *Xba*I site is marked with a solid line) under the following PCR conditions: KOD-plus DNA polymerase (Toyobo, Osaka, Japan) was used, and after initial denaturation at 98 °C for 1 min, a cycle of 98 °C for 15 s, 60 °C for 30 s and 74 °C for 30 s was repeated 25 times in TaKaRa PCR Thermal Cycler model TP2000. The PCR products were subjected to agarose-gel electrophoresis, and the gel was stained with ethidium bromide. The stained DNA fragments of a desired size were isolated and purified by using a Prep-A-Gene Purification Kit (Bio-Rad Laboratories, Hercules, CA) according to the manufacturer's protocol. The purified DNA fragments were digested with *Eco*RI and *Xba*I, and then ethanol precipitated. The DNA fragments corresponding to OR cDNA were then ligated with DNA Ligation Kit, version 2 (TaKaRa, Kyoto, Japan) into pTracer-EF A which had been digested with the same restriction enzymes.

2.3. Transformation of E. coli DH5α with pTracer-EF A/human OR cDNA

The plasmid bearing human OR cDNA was introduced into *E. coli* DH5α with a Gene Pulser (Bio-Rad) according to the manufacturer's protocols. Plasmid was extracted from positive clones, digested with *Eco*RI and *Xba*I, and subjected to agarose-gel electrophoresis to confirm the introduction of the cDNA to the pTracer-EF A vector. To further confirm that undesired mutations had not occurred, nucleotide sequences of both strands of the pTracer-EF A/OR-cDNA insert were determined using appropriate Cy5-labeled sequence primers listed in Table 1.

Table 1
Primers used for sequencing of human OR cDNA

Primer	Position	Nucleotide sequence
For pTracer-EF A		
pTA-R		5′-ACGACTCACTATAGGGAGAC-3′
pTA-U		5′-GGCTGGCAACTAGAAGGCACAGTCG-3′
For human OR cDNA		
OR-R1	362–385	5′-ACCTGAGCAGCCTGCCAGAGATCG-3′
OR-R2	915–939	5′-GGACATCTCGGACTCCAAAATCAGG-3′
OR-R3	1371–1390	5′-CATCGCCTCATCCTCCAAGG-3′
OR-U1	1800–1819	5′-GCTGGACGTAGACCTTGTGG-3′

2.4. Transfection of HepG2 cells with pTracer-EF A/human OR cDNA

Transfection of HepG2 cells with pTracer-EF A/OR-cDNA was performed by the lipofection method using Lipofectamine reagent (Invitrogen) according to the manufacturer's protocols. Briefly, pTracer-EF A/OR-cDNA was digested with *Sca*I, followed by ethanol precipitation, and the precipitate was dissolved in distilled water. The plasmid (3–6 μg) and Lipofectamine reagent (10 μl), both of which were diluted to 150 μl with William's E medium (Sigma Chemicals Co.) without fetal bovine serum (FBS) or antibiotics, were mixed and incubated for 30 min at room temperature. The resulting DNA–Lipofectamine complex was directly added to each dish. HepG2 cells were cultivated in Petri dishes (60 mm diameter, cell density of (1–2) × 10^6 cells/dish) in William's E medium containing 10% FBS (GIBCO), penicillin (100 units/ml)-streptomycin (100 μg/ml) (Sigma Chemicals Co.) at 37 °C for 24 h in an atmosphere of 5% CO_2. The cells were washed with the culture medium without FBS and antibiotics, and then mixed with the plasmid-Lipofectamine mixture described above, followed by cultivation for 48 h in the CO_2 incubator with culture medium exchange after 24 h.

Following the transfection, the transfected cells were subcultured in Petri dishes (100 mm diameter, cell density of 1.5 × 10^6 cells/dish). Twenty-four hours later, the culture medium was changed to one containing 100 μg/ml zeocine (Invitrogen), and zeocine-resistant HepG2 transfected cells were selected. The selected transfectants were subcultured in the medium containing zeocine (50 μg/ml). Hereafter, HepG2 transfectants stably expressing OR are referred to as HepG2/OR.

2.5. Western blot analysis

Western blot analysis was performed essentially according to the method of Guengerich et al. [9]. Whole-cell lysate fractions from HepG2/OR or HepG2 transfected with the plasmid having no OR cDNA (HepG2/mock) as well as a human liver microsomal fraction were subjected to SDS-PAGE using a slab-gel. Proteins on the gel were electroblotted onto a polyvinylidene difluoride (PVDF) membrane. In the case of OR, proteins were probed with goat anti-rat OR serum as a primary antibody (Daiichi Chemical Co.) and anti-goat IgG-alkalinephosphatase as a secondary antibody (Santa Cruz Biotechnology, Santa Cruz, CA). In the case of CYP2D6 and its variants, a monoclonal antibody raised against CYP2D6 (Daiichi Chemical Co.) were used as described previously [5].

2.6. Transfection of HepG2 cells with pcDNA3.1(+)/CYP2D6 or its variant cDNA

We previously prepared pBluescript II KS(+) bearing CYP2D6 cDNA or its various variants cDNAs (P34S, G42R, R296C and S486T) [5,10]. The plasmid bearing CYP2D6-WT or variant cDNA was digested with *Hin*dIII, and purified by agarose-gel electrophoresis as described above. pcDNA3.1(+) (Invitrogen) was also digested with *Hin*dIII, followed by dephophorylation of its 5′-terminus with calf intestine alkaline phosphatase to avoid self-ligation. The purified cDNA encoding CYP2D6-WT or its variant and pcDNA3.1(+), both of which were dissolved in TE buffer, were ligated at 37 °C for 12 h, followed by ethanol precipitation. The product was dissolved in sterile distilled water.

Transfection of HepG2/OR was performed by the lipofection method as described above. Seventy-two hours after starting the electroporation, trans-

fectants were selected in culture medium containing geneticin (600 μg/ml, Sigma Chemicals Co.). The selected transfectants were subcultured in the medium containing geneticin (200 μg/ml). Western blot analysis was performed as described above using a Human CYP2D6 Western Blotting Kit (Genetest, Seattle, WA). The HepG2 transfectants stably expressing OR and CYP2D6-WT are referred to hereafter as HepG2/OR/2D6.

2.7. Transfection of HepG2 cells with pTracer-EF A/CYP2D6 cDNA

CYP2D6-WT cDNA was introduced into pTracer-EF A as described for the introduction of OR cDNA into the same plasmid. The sites of *Eco*RI and *Xba*I and a Kozak sequence were introduced into CYP2D6 cDNA by PCR using the primers listed in Table 1. Transfection of HepG2 cells and selection of the resulting zeocine-resistant transfectants were performed as described above. The HepG2 transfectant expressing CYP2D6 but not exogenous OR thus obtained is referred to hereafter as HepG2/2D6.

2.8. Cultivation of HepG2 cells with DMSO or hemin

Hemin (15 mg) was dissolved with 0.5 ml of 1 M NaOH, and diluted to 1 mM with distilled water. The hemin solution was added to the culture medium at desired concentrations. HepG2 cells, HepG2/OR/2D6 and HepG2/2D6 ((6–7) × 10^6 cells per dish, three dishes for each CYP2D6 enzyme) were cultivated in the medium for 5 days. On day 6, the cultivation medium was changed to the medium with or without 0.1% DMSO or 5 mg/ml hemin, followed by further cultivation for 24 h, and then microsomal fractions were prepared from the whole cells on day 7.

2.9. Assay of enzymatic activities

Microsomal fractions as enzyme sources were prepared from HepG2 cells expressing OR and/or CYP2D6 or its variants. Cytochrome *c* reductase activity was assayed by the method of Omura and Sato [11]. Racemic BF 1″-hydroxylase activity was measured by the HPLC method reported previously [12]. Kinetic parameters (apparent K_m and V_{max} values) were estimated by analyzing Lineweaver–Burk plots using the computer program Prism version 4.0 software (GraphPad Software, San Diego, CA). Protein concentration was determined by the method of Lowry et al. [13].

2.10. Spectrophotometric analysis

HepG2 cells expressing OR and/or CYP2D6-WT ((6–7) × 10^6 cells per dish, three dishes for each CYP2D6 enzyme) were cultivated in the medium for 5 days. On day 6, the cultivation medium was changed to the medium with or without 0.1% DMSO, followed by further cultivation for 24 h, and then microsomal fractions were prepared from the whole cells on day 7. The fractions were diluted to a protein concentration of about 2 mg/ml with 100 mM potassium phosphate buffer (pH 7.4) containing 20% (v/v) glycerol. Total holo-CYP2D6 contents were spectrophotometrically measured as reduced carbon monoxide (CO) spectra according to the method of Omura and Sato [11] using 91 mM^{-1} cm^{-1} as absorption coefficient.

3. Results

3.1. Establishment of HepG2 transfectant stably expressing OR

Whole-cell lysates prepared from several lines of zeocine-resistant HepG2 cells that had been transfected with the OR gene were subjected to Western blot analysis using a polyoclonal rat OR antibody. As shown in Fig. 1, a clear protein band that immunochemically reacted with the antibody was observed in lanes 3–8, in which whole-cell lysate fractions were applied, and in lane 1, in which human liver microsomal fraction was applied. In lane 2, in which whole-cell lysate fraction of control HepG2 cells (HepG2) was applied, a faint protein band was observed.

From the transfectant whose whole cell lysate was applied to lane 3, the microsomal fraction was prepared and cytochrome *c* reductase activity was assayed. The activity was 116 units/mg protein, which was 4 times higher than that (27 units/mg protein) of the control HepG2 cell microsomal fraction. We therefore employed this transfectant having elevated cytochrome *c* reductase activity as a HepG2 cell line stably expressing OR (HepG2/OR).

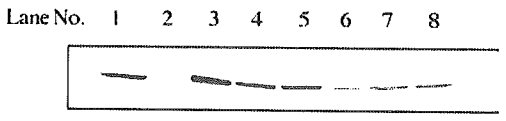

Fig. 1. Western blot analysis of OR protein in HepG2 cells transfected with human OR cDNA. Lane 1, human liver microsomes (15 μg); lane 2, HepG2 (1 × 10^5 cells); lanes 3–8, HepG2 tranfectants (1 × 10^5 cells).